AD_____

Award Number: W81XWH-07-1-0281

TITLE: Cellular Therapy to Obain Spine Fusion

PRINCIPAL INVESTIGATOR: Dr. Elizabeth Davis

CONTRACTING ORGANIZATION: Baylor College of Medicine, Houston, TX 77030

REPORT DATE: July 2012

TYPE OF REPORT: Final

PREPARED FOR: U.S. Army Medical Research and Materiel Command
Fort Detrick, Maryland 21702-5012

DISTRIBUTION STATEMENT: Approved for public release; distribution unlimited

REPORT DOCUMENTATION PAGE

Form Approved
OMB No. 0704-0188

1. REPORT DATE *(DD-MM-YYYY)*	2. REPORT TYPE	3. DATES COVERED *(From - To)*
01-07-2012	Final	1 Jul 2007 - 30 Jun 2012

4. TITLE AND SUBTITLE
Cellular Therapy to Obain Spine Fusion

5a. CONTRACT NUMBER

5b. GRANT NUMBER
W81XWH-07-1-0281

5c. PROGRAM ELEMENT NUMBER

6. AUTHOR(S)
Dr. Elizabeth Davis

E-Mail: edavis@bcm.tmc.edu

5d. PROJECT NUMBER

5e. TASK NUMBER

5f. WORK UNIT NUMBER

7. PERFORMING ORGANIZATION NAME(S) AND ADDRESS(ES)
Baylor College of Medicine
Houston, TX 77030

8. PERFORMING ORGANIZATION REPORT NUMBER

9. SPONSORING / MONITORING AGENCY NAME(S) AND ADDRESS(ES)
U.S. Army Medical Research and Materiel Command
Fort Detrick, Maryland 21702-5012

10. SPONSOR/MONITOR'S ACRONYM(S)

11. SPONSOR/MONITOR'S REPORT NUMBER(S)

12. DISTRIBUTION / AVAILABILITY STATEMENT
Approved for Public Release; Distribution Unlimited

13. SUPPLEMENTARY NOTES

14. ABSTRACT

Surgery of the spine to fuse the vertebral bones is one of the most commonly performed operations with an estimated 350,000 Americans undergoing this surgery annually with estimated costs of $60 billion. Current procedures are highly invasive with limited success. The goal of this study is to develop a safe efficacious system for inducing spine fusion which will eliminate the need for invasive surgery. We have currently developed a cell based gene therapy system that can induce rapid bone formation at a targeted location which is independent of immune status of the model. This system relies on adenovirus transduced cells expressing bone morphogenetic protein 2 to induce bone formation leading to vertebral fusion after delivery into the paraspinous musculature. To prolong cell survival and insure cells are maintained at the target site, we have encapsulated them in a non-degradable hydrogel material. This provides additional safety by eliminating direct injection of the virus through cell delivery, and prevention of cell diffusion, through encapsulation. Here we provide preliminary data; demonstrating spine fusion using this system at 6 weeks after induction. This is the first step in demonstrating efficacy, a critical component of preclinical testing. Thus with validation of our hypothesis, this approach can now be developed as a safe and efficacious gene therapy system for spine fusion, thus circumventing the need for costly invasive surgery.

15. SUBJECT TERMS
BMP2, Spine fusion, Hydrogel, Gene Therapy, Adenovirus.

16. SECURITY CLASSIFICATION OF:			17. LIMITATION OF ABSTRACT	18. NUMBER OF PAGES	19a. NAME OF RESPONSIBLE PERSON
a. REPORT	b. ABSTRACT	c. THIS PAGE			USAMRMC
U	U	U	UU	33	19b. TELEPHONE NUMBER *(include area code)*

Table of Contents

Introduction: Surgery of the spine to fuse the vertebral bones is one of the most commonly performed operations with some 400,000 Americans undergoing this type of surgery annually in the United States. The estimated cost associated with such procedures exceeding $60 billion annually demonstrating this to be a significant problem. In the most common form, posterolateral fusion, the paraspinous musculature is stripped and the bone decorticated, resulting in significant pain, reduced stability afforded by these muscles, and disruption of the blood supply to both bone and muscle. Further, success rates for fusion range from 50-70% depending on how many levels are fused and the number and types of attendant complications. We recently demonstrated that transduced cells expressing high levels of bone morphogenetic protein 2 (BMP2) in skeletal muscle could rapidly recruit and expand endogenous cell populations to initiate all stages of endochondral bone formation, with mineralized bone forming within one week of implantation. The central hypothesis of this application is that posterolateral spine fusion can be successfully achieved with only minimally invasive percutaneous techniques and without a scaffold, by collecting cells from patient's, transducing them to express BMP2, encapsulating the cells with hydrogel material, and then delivering them to the fusion site. If added structural stability is required, the injectable hydrogel will be crosslinked *in vivo* with a small fiber-optic light source. Successful completion of this project would advance the current state of gene therapy in this field by eliminating the search for an optimal osteoprogenitor cell and scaffolding.

Body: The central hypothesis of this application is that posterolateral spine fusion can be successfully achieved with a novel and simple minimally invasive percutaneous technique. We propose that this can be done by transducing human fibroblasts to express an osteoinductive factor (bone morphogenetic protein 2 or BMP2), encapsulating the cells with hydrogel material, and then delivering them to the fusion site. This injectable material will be a liquid, but once in place can be crosslinked with a small fiber-optic light source.
We have developed three specific tasks to accomplish our goals.

*** The experiments highlighted in blue are still being conducted as described in the original application, however, these were in overlap with another application and therefore no funds from this award were used or will be used for their completion.**

Task 1: *To determine the optimal levels of BMP2 for efficient rapid production of endochondral bone from human bone marrow mesenchymal stem cells (hBM-MSCs) transduced with a tetracycline regulated Ad5F35tet-BMP2 adenovirus carrying a red luciferase reporter gene.*

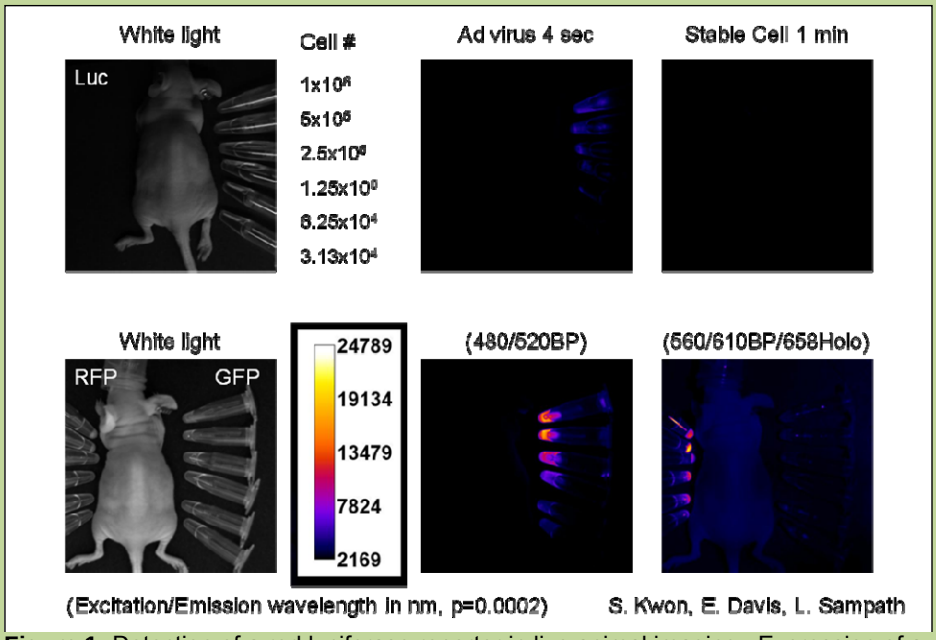

Figure 1: Detection of a red luciferase reporter in live animal imaging. Expression of a red shifted luciferase reporter was compared both in cells, and in live animals after subcutaneous intramuscular injection.Two types of cells were tested, one which was a cell line that had the reporter stably integrated, and the other cells which had been transduced with an AdCRBluc virus.

a. To determine if sustained expression of BMP2 is more efficient at inducing rapid bone formation than a pulse of expression using the tetracycline regulated vectors. **(Months 0-12)**

Comparison studies were performed to determine the optimal method for tracking transgene expression *in vivo*. As seen in figure 1, the originally described methodology using red luciferase reporter gene expression was compared to other red-shifted reporters to determine if we could obtain something more sensitive which would allow us to image the expression of the transgene during bone formation. In original experiments using luciferase (figure 1) we were unable to readily detect the reporter after intramuscular injection of our transduced cells at the levels routinely used for induction of bone formation. However, as seen in figure 2, when this was compared to dsRED, a red fluorescent protein, we could readily detect dsRED. Therefore we initiated studies using dsRED in place of the red luciferase.

In these studies, cells were transduced with Ad5dsRED (2500 vp/cell) and were encapsulated into microbead structures using PEGDA hydrogel (nondegradable). The microbeads were then injected into the hindlimbs of the animal, and transgene expression compared to animals receiving the same Ad5dsRED transduced cells which have not been encapsulated.

Two days after the initial injection of cells, dsRED expression was readily detected whether cells were encapsulated or not and in no cases were cells or microspheres detected migrating from the injection site (Figure 3A). The dsRED expression, as measured by fluorescence intensity at 590 ± 10 nm, was significantly elevated in microencapsulated Ad5dsRED-transduced cells compared to other groups (Figure 3B). Microencapsulated control cells transduced with AdEmpty cassette had no fluorescent signal at 590 ± 10 nm, demonstrating that neither the cells nor the PEGDA were autofluorescing. Fluorescent intensity in animals receiving Ad5dsRED-transduced cells directly injected was substantially reduced after seven days and was indistinguishable from control. In microencapsulated Ad5dsRED-transduced cells, this 590 ± 10 nm dsRED fluorescent signal was significantly elevated over that of microencapsulated control cells for 15 days (Figure 3B). After 15 days, these levels dropped; however, signal was still detectable (Figure 3A, arrows) in some animals, suggesting that the microencapsulated cells remained viable to express the dsRED transgene. Statistical power to detect intensity over control ranged from 100% in microencapsulated cells to 99.7% in directly injected cells, and power to detect the difference between microencapsulated and unencapsulated cells was 88%.

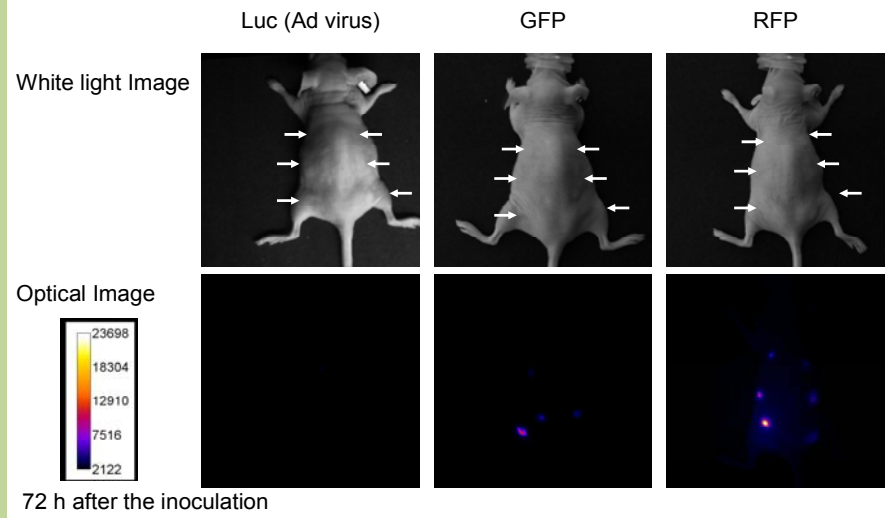

Figure 2: Comparison of reporter expression after intramuscular injection of dsRED, GFP, and CRBluc in live animals, through optical imaging.

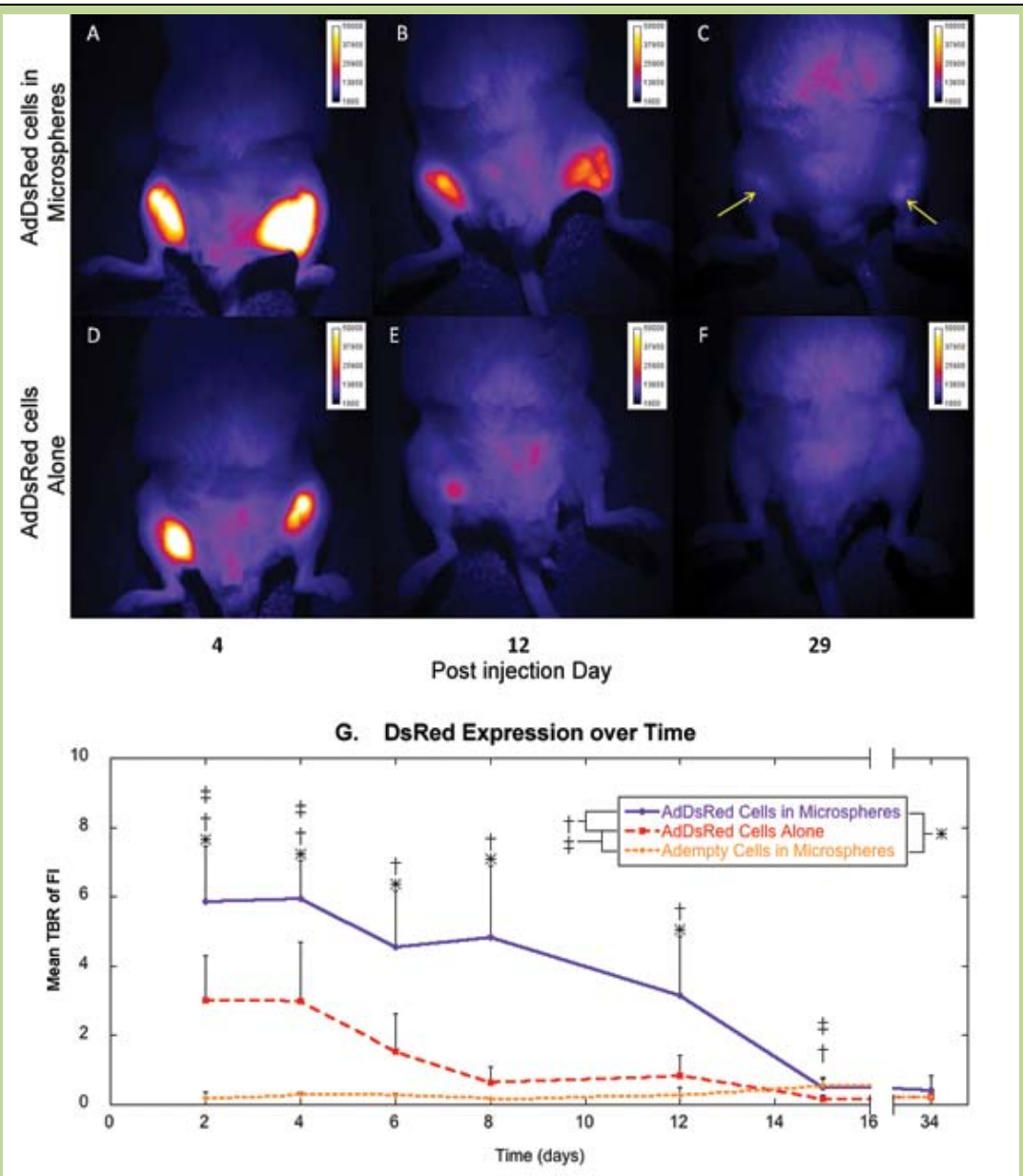

Figure 3: Optical fluorescence imaging of mice injected with cells expressing dsRed. Top panels (A through C) are images of a representative mouse (n=4) injected with dsRed-expressing cells encapsulated in microspheres and bottom panels (D through F) are of a mouse injected with dsRed-expressing cells directly, without microspheres. The images were taken at day 4, 12 and 29 post-injection of cells. By day 29, the fluorescent signal is at background levels or undetectable for the mouse given dsRed-expressing cells without microspheres (F). Whereas, the signal remains detectable in the mouse given dsRed-expressing cells encapsulated in microspheres (C).
G. Mean Target-to-Background Ratio (TBR) of Fluorescence Intensity (FI) in mice given unencapsulated dsRed cells, microencapsulated dsRed cells or microencapsulated control cells. * $p \leq 0.05$ for microencapsulated dsRed cells versus microencapsulated control cells; † $p \leq 0.05$ for microencapsulated dsRed cells versus unencapsulated dsRed cells; ‡ $p \leq 0.05$ for unencapsulated dsRed cells versus microencapsulated control cells.

b. To determine the optimal expression time of BMP2 from cells embedded in hydrogel for the production of rapid bone formation. **(Months 9-12)**

We next set up similar experiments to track the dsRED in live animals during heterotopic ossification. In these experiments, we transduced the cells with an Ad5BMP2-dsRED virus, which was not tetracycline regulated. In these studies we look at the ability to detect the signal through the bone matrix that is forming. As seen in figure 4, dsRED could readily be detected above background for up to 16 days. As expected the microbeads were detected for a much greater period than the directly injected cells, with the majority of the expression from the directly injected cells being suppressed within 6 days whereas the transgene expression from the cells encapsulated in the microbeads was detected for 15 days, with one animal going out as long as 30 days. The new bone co-registered with the location of the microbeads, confirming the histological findings that the bone is forming immediately around the microspheres, or injected cells.

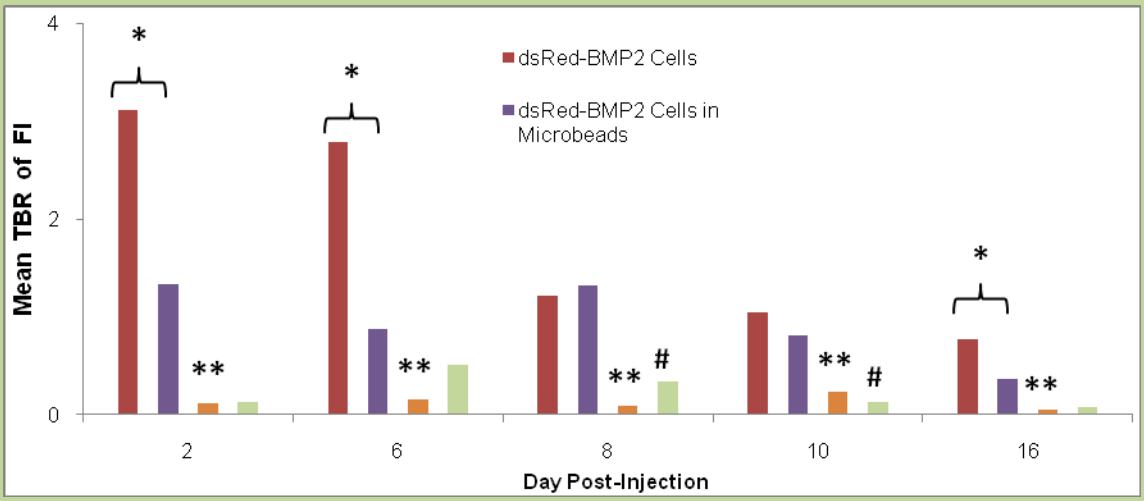

Figure 4: Mean Target-to-Background Ratio (TBR) of Fluorescence Intensity (FI) in mice given unencapsulated dsRed cells, microencapsulated dsRed cells or microencapsulated control cells.
*P < 0.05 for Ad5dsRED-BMP2 transduced cells versus Ad5dsRED-BMP2 cells in microbeads at days 2, 6, and 16 post-injection.
**P < 0.05 for Ad5dsRED-BMP2 cells transduced cells versus Ad5dsRED-BMP2 cells in microbeads at all time points.
# P < 0.05 for dsRED-BMP2 cells in microbeads versus Ad5empty cassette transduced cells (Control) in microbeads at days 8 and 10 after injection.

Since it appeared that changing the timing of BMP2 expression within the animal did not affect the bone formation, we next looked at the level of BMP2 expression within the local area in comparison to new bone formation. Using a rat fibula model, we transduced cells to express BMP2 and calculated the level of BMP2 protein secreted into the media. We then injected escalating numbers of cells, to increase the level of BMP2 protein in the local area. As expected there was a threshold level of BMP2 that was required for any bone formation, however, once above this, bone formation occurred at the same rate, in regards to maturation, density, mineral content. However, we did observe a significant change in the volume of bone made, where it increased with dose, and eventually hit a second threshold which was the maximum amount of bone that could be produced within the location. This is presumably due to saturation of BMP2 receptors within the area. Since BMP2 functions by establishing gradients, which most likely lead to cell migration towards the concentration that permits cellular differentiation, the edge of the bone will be defined by the gradient of BMP2, with more bone being made when higher levels of BMP2 are produced and can establish higher concentrations of BMP2 in a larger region. Alternatively the same bone is produced at much smaller amount, when the required concentration of BMP2 for cell differentiation/migration only involves a tiny region. This information is critical for targeted exactly where the bone should be produced. We are currently calculating the distance of the edges of the bone from the cells themselves, with correlation to concentrations of BMP2, to produce a "map" of where the new bone will be formed. With the ability to follow bone formation optically/radiologically, we can then confirm our maps. We have actually completed the analysis of optimal BMP2 expression, and this aim.

b. To demonstrate spine fusion using Ad5F35tet-BMP2 transduced cells encapsulated in hydrogel can effectively lead to spine fusion **(Months 0-12).**

We have been working on spine fusion in the mice using the directly injected cells (see task 3 and appendix). **This work is completed for mice.** We are now focused on completing fusion studies with the microspheres, in the rat using both the degradable and non-degrable forms of the hydrogel. **See next subaim.**

c. To demonstrate regulated expression of BMP2 in spine fusion studies using an Ad5F35tet-BMP2-IRESCBRLuc vector in which expression can be tracked through live animal imaging. **(Months 12-24)** We have already determined that there is a threshold level of BMP2 that is required for bone formation, and extending the time of production of the BMP2 does not change the formation of bone (Lazard *et al*, 2011). **See next sub aim**.

d. To track the BMP2 delivery cells *in vivo* during spine fusion by following the luciferase expression via live animal imaging. **(Months 24-48). See above section.** We are currently performing these studies in rats to track spine fusion using the microspheres, following an IFP reporter. This reporter is within the near infrared, and appears to be able to penetrate the bone more effectively. Further, the background is very low, allowing us to really pinpoint where the transgene is being expressed. In these experiments we have also included an Alexafluor dye within the hydrogel material so we can track both reporters and co-localize transgene expression, microsphere-polymer, and new bone formation. These experiments are ongoing and should be completed in the next 3 months, under our requested no cost extension.

Task 2: To design an optimal hydrogel material that will rapidly promote endochondral bone formation and be capable of removal through bone remodeling processes. In addition to BMP2 transduced cells, we propose to include peptides essential to the recruitment and migration of osteoprogenitors for bone and cartilage. Selective protease sites will also be introduced into the hydrogel to allow for osteoclast selective degradation during bone remodeling. We propose to do this by incorporation of calcium into the material and inclusion of cathepsin K protease cleavage sites into the material. Inclusion of these factors in the hydrogel will provide a mechanism for removal of the hydrogel once bone has formed by using the normal bone remodeling process.

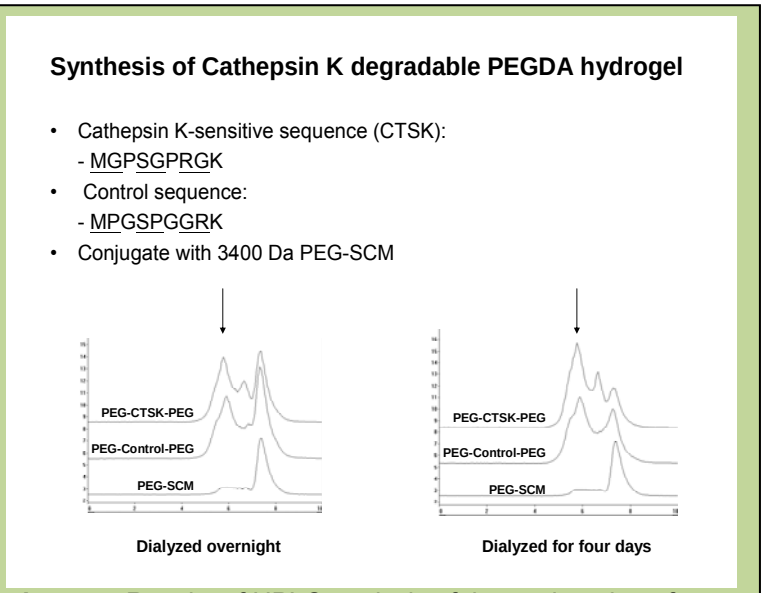

Figure 5: Results of HPLC analysis of the conjugation of peptide with the PEGDA hydrogel

a. Optimize and develop a hydrogel that can be specifically degraded by osteoclasts. **(Months 0-24)**

For more details please see reference (Hsu *et al,* 2011). We have synthesized the peptide MGPSGPRG using a 431A solid-phase peptide synthesizer (Applied Biosystems, Foster City, CA). In order to make degradable PEG, we start with PEG-DA-SMC (succinimidyl carbonate). The PEG-SMC is conjugated with our peptide in order to get PEG-PEPTIDE-PEG. So, we expect to obtain three peaks representing the completely conjugated product: PEG-PEPIDE-PEG, incompletely conjugated product: PEG-PEPTIDE and unconjugated product: PEG-SMC (Figure 5). We have run GPC tests on it and the results indicate that there is still unconjugated PEG, ie: we have PEG-Peptide or free PEG in the preparations. We have tried changing the ratio of peptide to PEG, changing the length of conjugation time, increasing the pore size of the dialysis membrane and changing the length we dialyze the conjugation

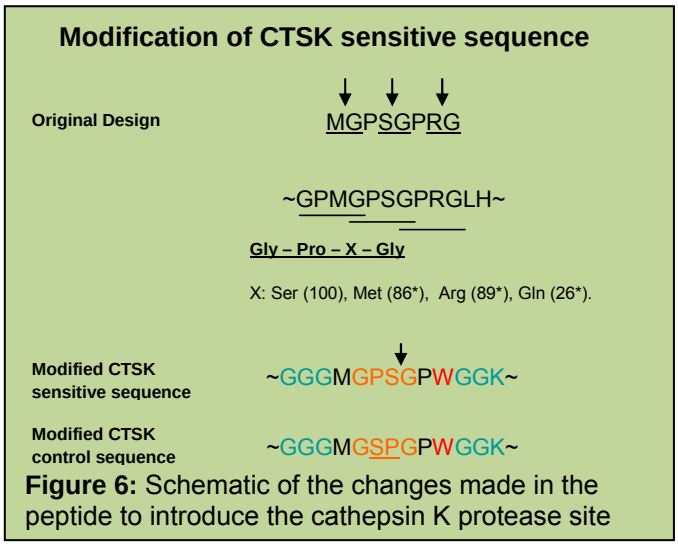

Figure 6: Schematic of the changes made in the peptide to introduce the cathepsin K protease site

products. These have led to a higher concentration of PEG-PEPTIDE-PEG as indicated by the GPC results (Figure 5). We have cathepsin K (Calbiochem; Cathepsin K, His•Tag®, Human, Recombinant, *E. coli*). Degradation tests have found that the material did not degrade as expected. Analysis of the materials suggested that the protease site may be too confined to actually bind enzyme for digestion, thus, the protease site was redesigned to have a longer amino acid sequence linker to allow for better digestion. Thus the modified peptide sequence is GGGMGPSGPWGGK, see figure 6.

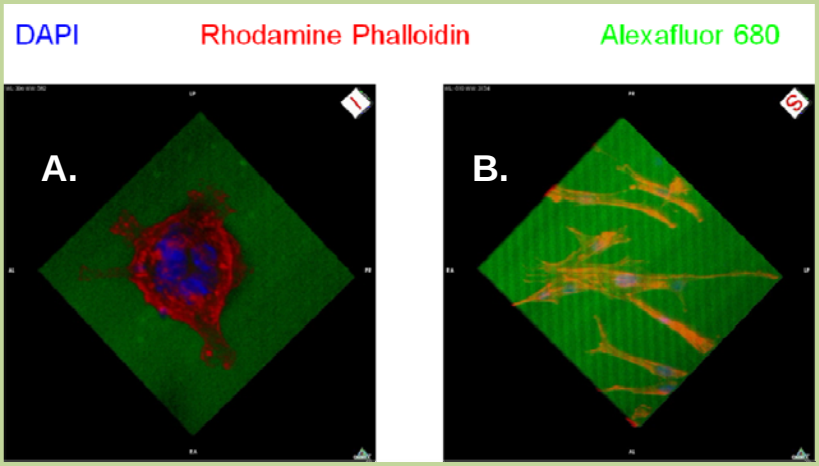

Figure 8: Three-dimensional fluorescent image reconstruction of an active osteoclast on the GPSG hydrogel surface. The GPSG hydrogel was labeled with Alexafluor 680 fluorophore (green), which is conjugated with the acryloyl-PEG-RGDS and incorporated into the hydrogel by photo-polymerization. The cells were fixed and permeabilized before staining the nuclei with DAPI (blue) and F-actin by rhodamine phalloidin (red) 48 hours after seeding. (A) Composed z-stack images of the osteoclast on hydrogel. (B) Composed z-stack images of osteoblasts on hydrogel. Osteoblasts did not appear to leave any pits.

We next examined the ability of the cathespin K sensitive hydrogels to dergade in the presence of the enzyme. The hydrogels with the cathepsin K sensitive peptide GGGMGPSGPWGGK were designed to carry a cathepsin K sensitive cleavage site between serine and proline. Proteinase K was used as a positive control. While the gel degrades, the peptide that was incorporated into the hydrogel structure will be cleaved by enzymes and gradually release into solution. The degradation profiles of GPSG hydrogels were measured by monitoring the concentration change of tryptophan in solution at UV absorbance of 280 nm. Crosslinkable GPSG hydrogels were polymerized in microcuvettes and incubated with enzyme solutions. After equilibilium swelling in TBS overnight, hydrogels were treated with different enzymes to evaluate the degradation profiles (Figure 7). After incubation with different enzyme solutions for 24 hours, hydrogels in cathepsin K and proteinase K solutions has similar degradation profiles, both indicating a rapid tryptophan concentration increase within the first hour and reaching about 80% release of total tryptophan at 24 hours. No degradation was

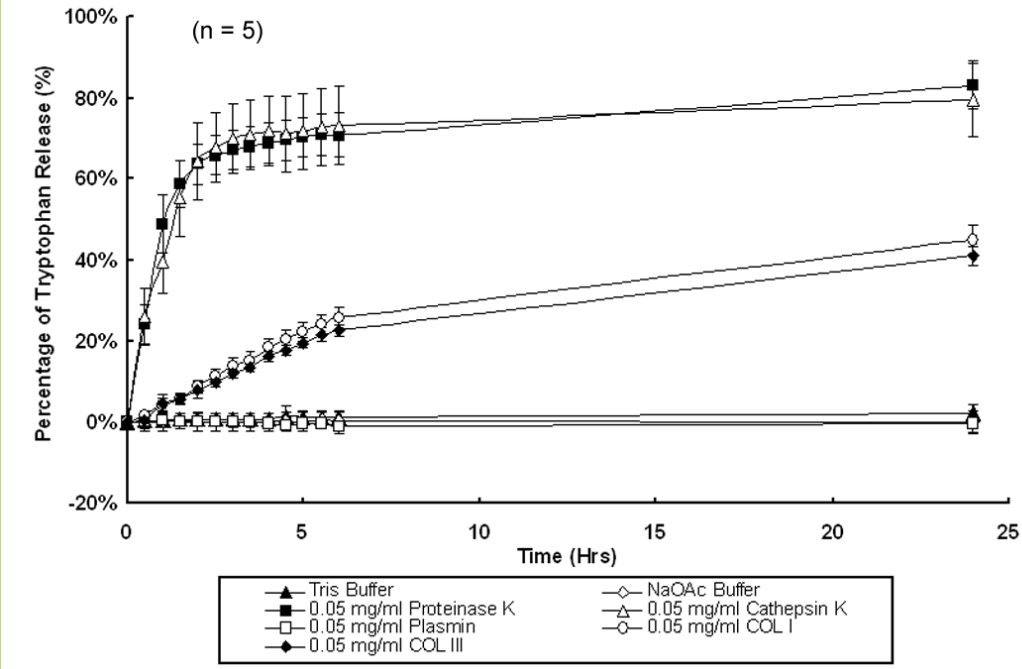

Figure 7: Degradation profiles of cathepsin K-sensitive GPSG hydrogels. Hydrogel droplets (3 µl) were polymerized in each micro-cuvette and swelled overnight with 250 µl of TBS buffer. Each hydrogel was incubated in buffer or enzyme solution at 0.05 mg/ml at 37^{O}C. UV absorbance at 280 nm was measured over 24 hours to monitor tryptophan release corresponding to the degradation of the GPSP hydrogels.

observed when hydrogels were incubated in TBS buffer, NaOAc buffer, and plasmin. Hydrogels incubated in nonspecific collagenase I and collagenase III solutions also released 40% of incorporated tryptophan after a 24 hour incubation (figure 7).

We next tested the degradable hydrogel to determine if it could be selectively degraded by osteoclasts. Raw 264.7 cells were differentiated in culture medium containing 30 ng/ml RANKL for 4 days. Cells collected through gradient centrifugation and placed in culture where they were enzymatically stained for tartrate acid phosphatase activity (TRAP). Multinucleated cells in the culture appeared to stain positive for TRAP suggesting that they had ungoing osteoclast differentiaiton. The majority of cells at the bottom fraction of the gradient contained the TRAP+ dRAW 264.7 osteoclasts were then used for hydrogel degradation studies. To demonstrate the ability of the cells to both adhere to the hydrogel material so a normal substrate for growth, as well as have the selectivity in degradation, we next plated both primary osteoblasts and the TRAP+ dRAW264.7 osteoclasts onto GPSG hydrogel sheets containing the RGD binding sites which were preformed, to provide a smooth surface to ensure they do not possess imperfections other than those introduced by degradation from the cell populations.

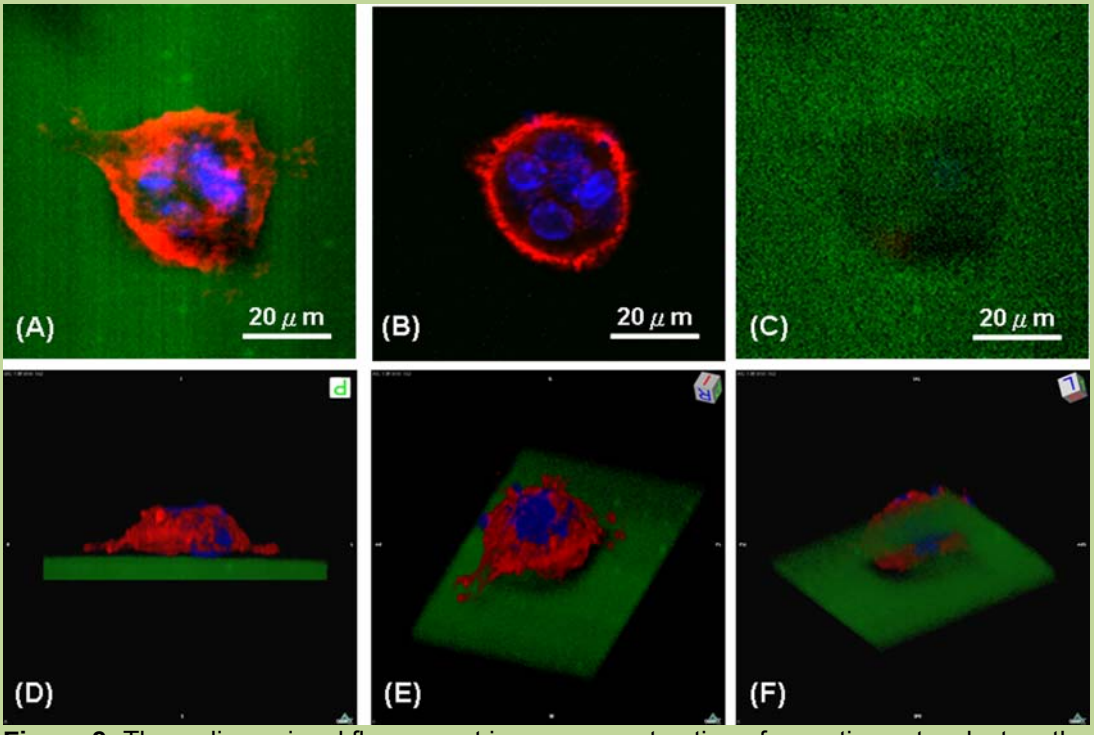

Figure 9: Three-dimensional fluorescent image reconstruction of an active osteoclast on the GPSG hydrogel surface. The GPSG hydrogel was labeled with Alexafluor 680 fluorophore (green), which is conjugated with the acryloyl-PEG-RGDS and incorporated into the hydrogel by photo-polymerization. The cells were fixed and permeabilized before staining the nuclei with DAPI (blue) and F-actin by rhodamine phalloidin (red) 48 hours after seeding. (A) Composed z-stack images of the osteoclast and hydrogel. (B) Sealing ring and multiple nuclei of the osteoclast. (C) GPSG hydrogel with fluorescent signal lost at middle. Z-stack Images were reconstructed using the volume renderings algorithm and presented from (D) side view, (E) orthogonal view from above, and (F) from bottom. The resorption site is located underneath the osteoclast, which was can be observed in the loss of the fluorescent intensity of Alexafluor 680. The resorption pit on the hydrogel surface can be clearly seen from different angles, suggesting that the GPSG hydrogel has been degraded by cathepsin K secreted by osteoclasts.

As can be seen in figure 8, both cell types readily adhered to the material, and formed normal cell structures observed in tissue culture. The degradable or GPSG hydrogels possessing Alexafluor 680 (green color) were fixed and stained with DAPI (blue color) for nuclei and rhodamine (red color) phalloidin for F-actin in the cytoplasm. As can be seen in figure 8 and 9, observed on hydrogel surface were actual resorption pits generated by RAW264.7 osteoclasts which were absent on the GPSG hydrogels which had been seeded with osteoblasts. Hydrogels-osteoclasts interactions were examined under confocal microscopy at higher magnification. Multinuclear and polarized cells RAW264.7 osteoclasts were identified on the hydrogel surface, (Figure 9A). A sealing ring of F-actin and multiple nuclei were clearly observed (Figure 9B). On the hydrogel surface where the osteoclast was located, a decrease in the fluorescent signal was observed (Figure 9C). The z-stack images were then examined closely by three-dimensional reconstructions using a volume rendering method. Figure 9D is the side view, showing the osteoclast attached to the hydrogel. From the three-dimensional perspective of the image from the top (Figure 9E) and bottom (Figure 9F) of the hydrogel, the loss in fluorescent signal of the hydrogel reveals a hole

in the hydrogel through which the cell can be seen. This signal loss is indicative of activity by the differentiated RAW264.7 osteoclasts, degrading the underlying hydrogel and creating a pit, resulting in the fluorescent intensity loss. No signal loss was observed on the gels seeded with dMC3T3-E1 cells. Therefore it appears that the osteoclasts may be selectively able to remodel the hydrogel material as predicted.

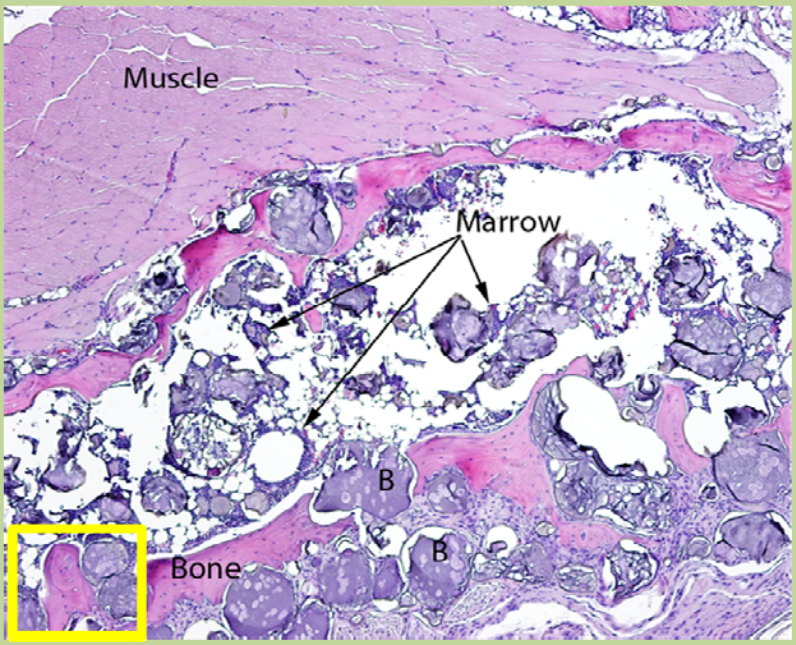

Figure 10: Photomicrograph of a hematoxylin and eosin stained tissue section depicting the degradation of the microbeads *in vivo.*

We next tested the material *in vivo* to determine if we observed degradation, and replacement of the microspheres with bone. We injected the microspheres, and then approximately 3 weeks after injection harvested the tissues, processed, and sectioned through the newly formed heterotopic ossification to detect the microspheres. Figure 10 shows a representative photomicrograph of a hematoxylin and eosin stained section of heterotopic bone and bone marrow. Intact microspheres can be detected within this section; however, there are also microspheres within the maturing bone that appear to be degrading. Further, the yellow rectangle encompasses a region which appears to be newly formed heterotopic bone, in the shape of a microsphere, suggesting that the removal of that material may be complete at this time. We are currently completing this *in vivo* analysis by following the samples out longer term, to determine if we can come to complete degradation of the material and remodeling of the bone.

b. *Engineer cellular binding sights within the hydrogel to determine if this improves, cell viability of the transduced cells, and in turn BMP2 expression, and to tentatively enhance the migration of mesenchmyal stem cells to the sight of bone formation.* **(Months 24-36)**

We have introduced RGD binding sites within and throughout the hydrogel to enhance binding of the osteoclasts (see above section) as well as other cell migration. This has been very effective in allowing cells to bind to the material, during bone formation. Additionally, inclusion of the RGD binding sites within the material has appeared to greatly enhance cell viability, allowing for the cells to remain viable. However, the most optimal improvement for BMP2 expression and cell viability has come from altering the structures to be microspheres, rather than larger beads (Bikram *et al*). Comparison of the BMP2 secretion from larger hydrogel structures to the microbead structures, showed a significant improvement. Figure 11 shows the BMP2 expression from larger bead structures, in comparison to the cells which were not encapsulated (Plated cells). As seen in Figure 11, the BMP2 expression is reduced by 50% in culture supernatants isolated from the encapsulated cells within the bead structures, as compared to the plated cells.

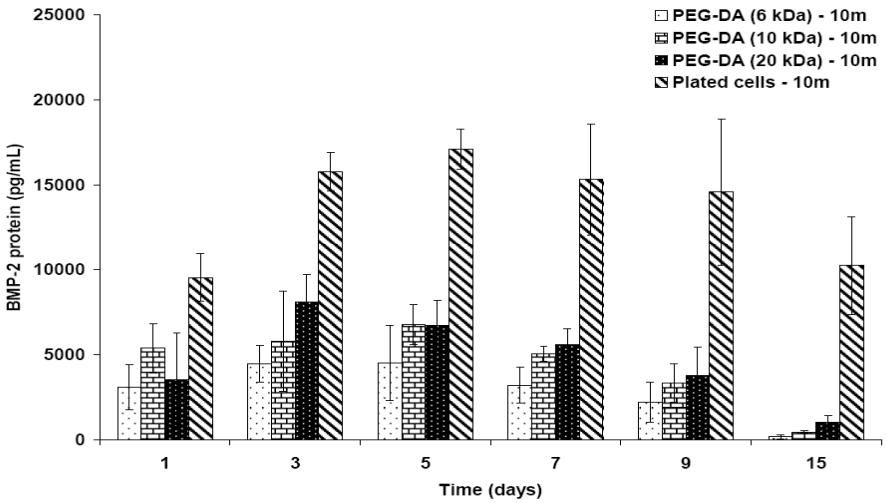

Figure 11: Western blot analysis for the detection of secreted BMP-2 protein. (a) Human recombinant BMP2 (lane 1), conditioned medium from PEG-DA (10 kDa) hydrogels only (lane 2), conditioned medium from 10 million MRC-5 cells encapsulated within PEGDA (10 kDa) hydrogels (lanes 3 and 4), conditioned medium from 10 million transduced fibroblasts control (lanes 5–8), human recombinant BMP-2 (lane 9), conditioned medium containing secreted BMP-2 protein from 10 million transduced fibroblasts encapsulated within PEG-DA (10 kDa) hydrogels (lanes 10–17). (b) Alkaline phosphatase activity in W20-17 cells without the addition of conditioned medium (W20-17) and after addition of conditioned media from PEG-DA (10 kDa) hydrogels with 10 million transduced fibroblasts and control plated transduced fibroblasts (Days 1–15). Data reported as mean ± SD, n = 5.

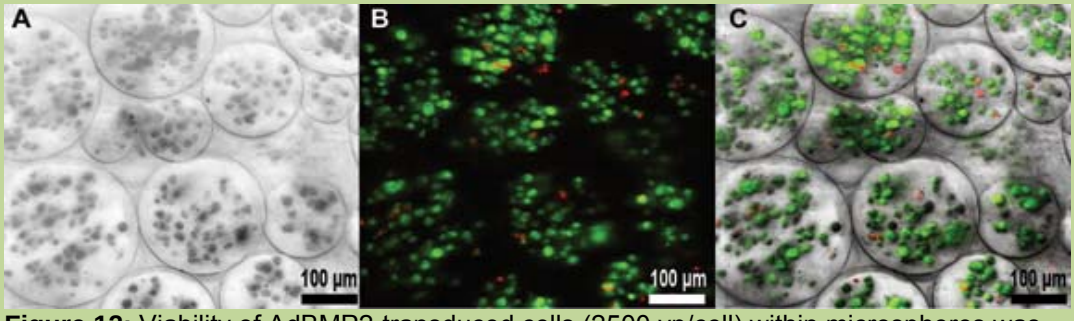

Figure 12: Viability of AdBMP2-transduced cells (2500 vp/cell) within microspheres was assessed at day 7 using a LIVE/DEAD® Viability/Cytotoxicity Kit for mammalian cells (Invitrogen, Molecular Probes, Eugene, OR). **A.** Minimum intensity projection of a differential interference contrast (DIC) Z-stack. **B.** Maximum intensity projection of fluorescent Z-stack merge of red and green channels. The red channel was thresholded to eliminate diffuse virus staining. Dead cells appear red and live cells appear green. **C.** Overlay of panels A and B. Living cells accounted for 95.08% ± 0.47% of total cells encapsulated.

We chose to next re-engineer the encapsulated structures, into microspheres, which hold between 0-100 cells (Olabisi *et al*, 2011a). As seen in figure 12, within the microspheres, live cells converted the non-fluorescent calcein AM into green fluorescent calcein while ethidium homodimer freely passed through the permeable membranes of dead cells to bind the DNA and fluoresce red. Encapsulated cells showed high viability 95 ± 0.5 %, suggesting that they were not adversely affected by the microencapsulation process.

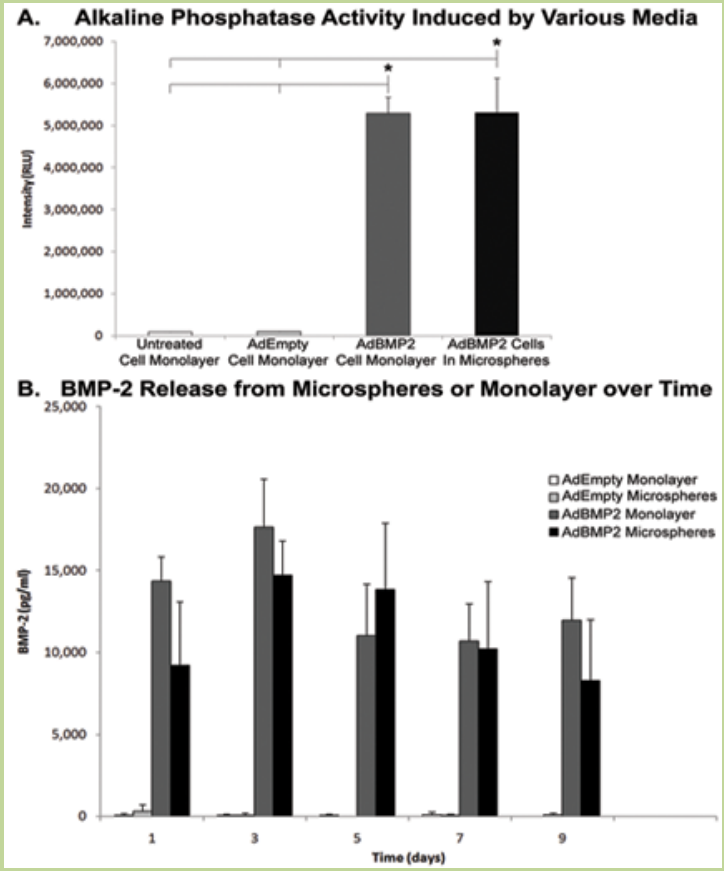

Figure 13: Comparison of BMP-2 expression, secretion and activity after PEGDA encapsulation. **A.** BMP-2 protein in culture supernatant taken from AdBMP2- or AdEmpty cassette-transduced cells (25000 vp/cell) (monolayer), or those encapsulated in PEGDA microspheres was quantified by sampling every other day for 9 days and evaluated using an ELISA. **B.** Alkaline phosphatase activity in W20-17 cells after addition of conditioned media from AdBMP2- or AdEmpty cassette-transduced cells (25000 vp/cell) (monolayer), or AdBMP2-transduced cells encapsulated in PEGDA microspheres. As a negative control, we also included culture supernatant from untransduced cells. Alkaline phosphatase activity is depicted as the average relative chemiluminescence units (RLU), where n=3. Error bars represent means ± SD for n=3. A Student t-Test was applied to demonstrate significance. AdBMP2-transduced monolayer and microsphere groups had significantly greater alkaline phosphatase activity and BMP-2 concentration levels ($p < 0.05$) when compared against other groups, but no differences when compared to each other. In other words, microencapsulation had no effect on BMP-2 release and function.

We also compared the level of BMP2 in culture supernatant taken from both cells directy plated and cells encapsulated in microspheres. BMP2 activity was quantified by measuring alkaline phosphatase (AP) activity in W20-17 cells exposed for 72 hours to the culture supernatants from AdBMP2-transduced cells directly plated or encapsulated in microspheres was significantly elevated over control cells but there was no difference between these groups, indicating the BMP-2 released is functionally active (Figure 13A). A 9 day time course of BMP-2 levels in culture supernatant was quantified by ELISA to be approximately 17,500 pg/ml and 15,000 pg/ml for directly plated and microencapsulated cells, respectively (Figure 13B). No BMP-2 was detected in either culture supernatant from AdEmpty cassette-transduced cells, or control cells. The results suggest that the smaller structures, may allow for both greater cell viability and diffusion of BMP2.

MicroCT analysis of bone formation showed a significantly greater volume of heterotopic ossification in tissues receiving microspheres (Figure 14A, C) than those receiving directly injected cells (Figure 13B, D). Statistical power to detect differences between volumes formed in these groups was 72.5%. Cross-sectional microCT analysis of the newly formed bone revealed a similar architecture between the groups. Heterotopic bone formed by both the microencapsulated cells and directly injected cells had a pattern of dense bone surrounding a hollow interior (Figures 14C and D); however the circumference of bone within the directly injected cells was significantly smaller. Microencapsulated AdBMP2-transduced cells produced approximately twice the bone volume of unencapsulated cells (Figure 15B). Despite the volumetric increase, the bone tissue mineral content was statistically similar between these groups, although trending towards an elevation in samples that received the microspheres (Figure 15A). This corresponds with the change in tissue mineral density of the new bone surrounding the microspheres (Figure 15C). The newly formed bone appears to be slightly less dense, leading to the overall similarity in mass between the two groups. Statistical power to detect differences between bone densities in these groups was 76.7%.

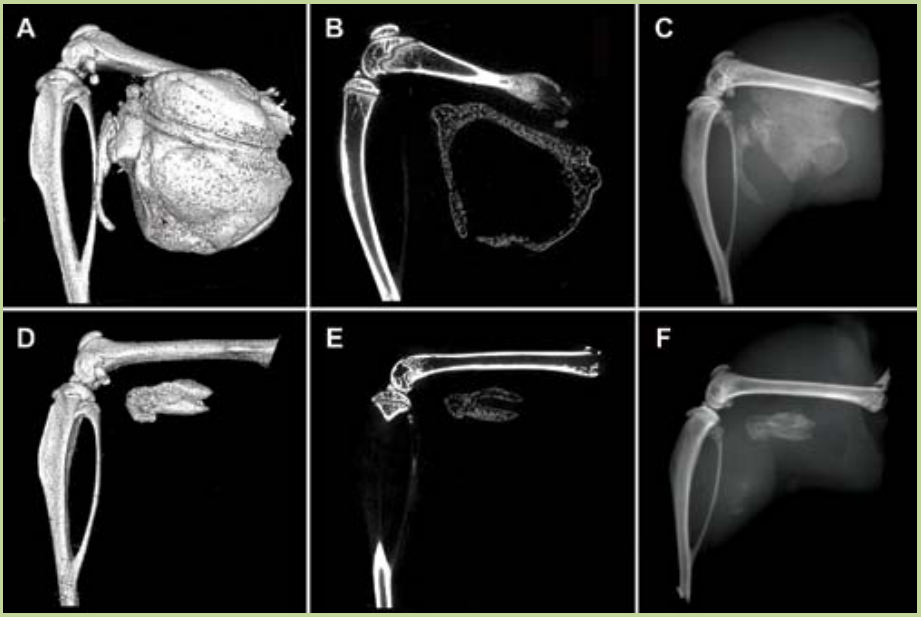

Figure 14: Micro computational analysis of the resultant heterotopic bone formation. Left images (**A, D**) are 3D surface renderings of the resultant heterotopic bone, while middle images (**B, E**) are cross-sectional slices through the new bone. Right images (C, F) show corresponding radiograms. Panels A - F show the resultant mineralization of the muscle tissues after injection of AdBMP2-transduced cells (2500 vp/cell) encapsulated into PEGDA microspheres (**A - C**) or direct injection of unencapsulated AdBMP2-transduced cells (**D - F**). Both have a denser rim of bone, with a hollow interior structure, suggesting that the biomaterial did not alter bone patterning.

From histological analysis, both groups had significant new bone formation within the muscle (Figure 16). In tissues that had received the direct injection of AdBMP2-transduced cells, there was a small compact piece of bone forming a ring-like structure encircling what appears to be blood and tentative stroma, and just exterior to this structure was significant adipose (Figure 16A). A similar structure was observed in tissues that had received microspheres (Figure 16B). Since the microspheres did not degrade, they appear histologically as gaps or holes within the matrix (Figure 16B). Thus, despite the presence of nondegradable microspheres, both structures were patterned to have a dense bone structure with a bone marrow-like cavity on the interior. Thus although the inclusion of the RGD is critical for osteoclast resorption of the materials, the essential component of the hydrogel materaisl for optimal bone formation appears to the encapsulation procedure and to maintain smaller structures (microbeads) possessing 0-100 cells, and allowing for better diffusion of nutrients and factors throughout the cell pellet, enhancing both transgene expression and cell viability.

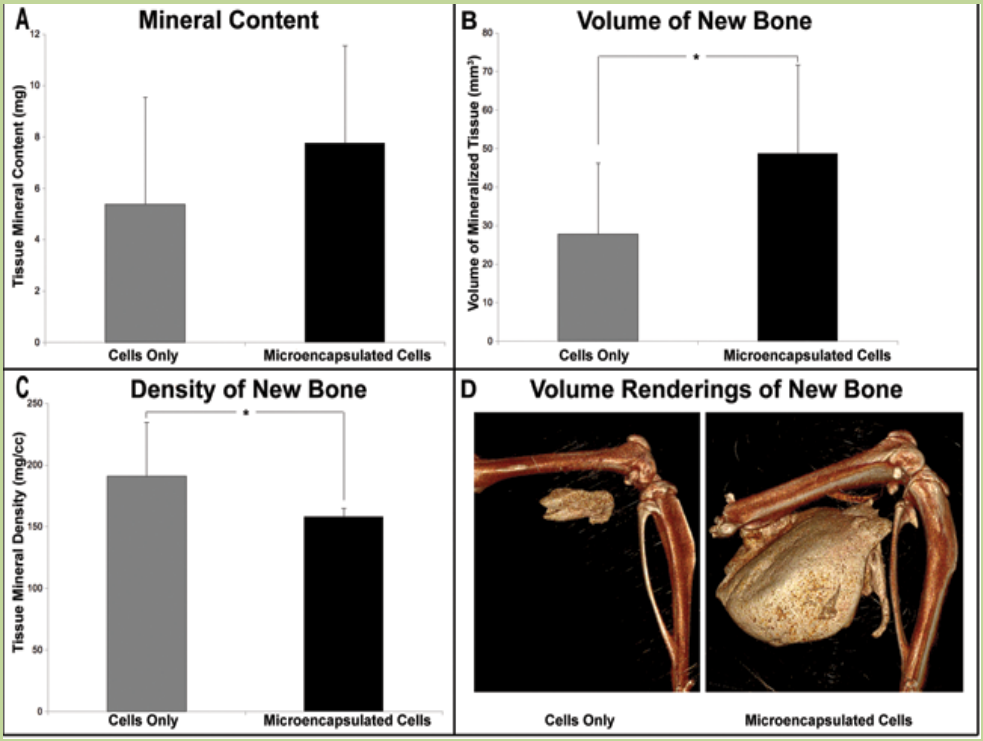

Figure 15: Quantification of the heterotopic ossification using microcomputational analysis. Cells were transduced with AdBMP2 and either directly injected or encapsulated into microspheres prior to injection, and the resultant heterotopic bone was analyzed two weeks later. Tissue parameters: **A.** bone tissue mineral content, **B.** bone volume of mineralized tissue, and **C.** bone tissue mineral density were calculated for the newly formed bone (n=6 per group). The means and standard deviations for each group were calculated and compared using a one-way analysis of variance. Results indicate that mineral content is statistically equivalent (p=0.2) between the groups, whereas the AdBMP2-transduced cells in microspheres had a significantly greater volume (p=0.038) than the AdBMP2-transduced cells directly injected. Alternatively, the bone tissue mineral density was significantly denser for the group receiving the cells directly as compared to those in microspheres (p=0.029). Panel **D.** shows a 3D volume rendering of new bone formed in cell only and microencapsulated cell groups, respectively.

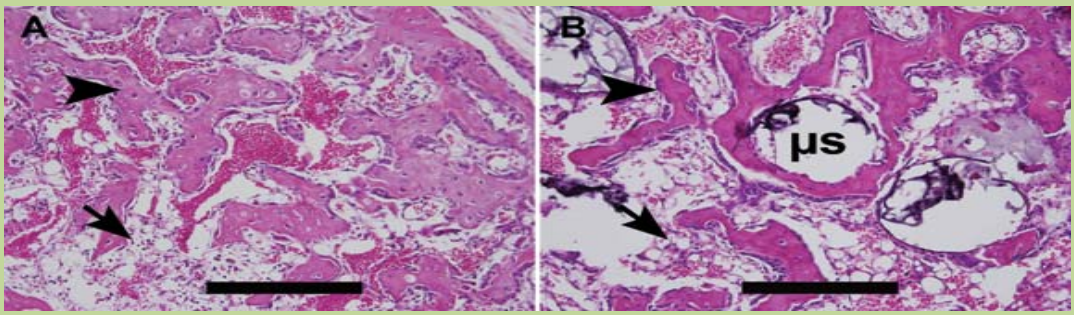

Figure 16: Photomicrographs of heterotopic ossification. Hematoxylin and eosin stains of new bone formation by: **A.** directly injected and **B.** microsphere (μs) encapsulated cells. Both groups show small compact pieces of bone (arrowheads) forming ring-like structures, encircling what appears to be blood and tentative stroma in the inner region, with significant adipose (arrows) just exterior to the new bone. Scale bars are 500 μm.

c. *Engineer proteins that may enhance the BMP2 bone inductive response, such as VEGF-A or -D and compare with gels without additional proteins.* ***(Months 36-48)***

We have demonstrated that the BMP2 rapidly induced new vessel formation, and elevates expression of VEGFs within the localized region of bone formation. Addition of the proteins to the material does not rapidly enhance the bone formation. As mentioned in the previous section, analysis of the newly forming bone shows a strong patterning of the bone formation even with the microspheres. The inside of the bone possesses a normal vascularized bone marrow cavity, amongst the microbeads.

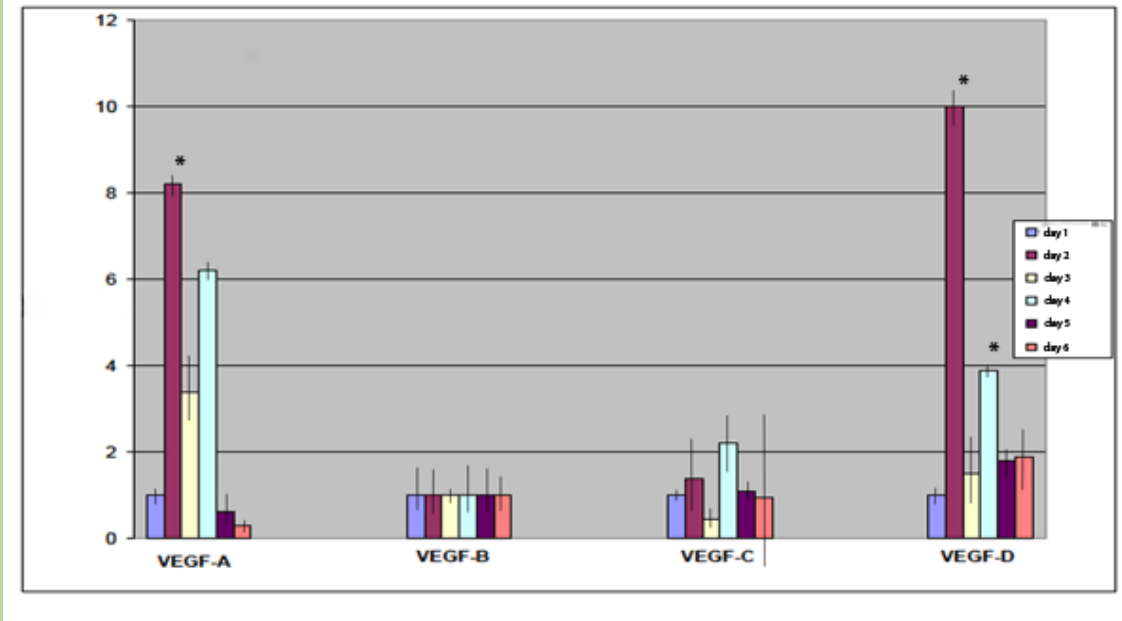

Figure 17: Quantitative RT-PCR of mRNA of VEGF family members within tissues isolated surrounding the site of new bone formation over daily intervals. n=8 biological replicates, and n=4 experimental replicates). The data is represented as a ΔΔ Ct.

We recently demonstrated the rapid increase of VEGD and A, within 48 hours of delivery of the BMP2. Interestingly this gene expression of these proteins within the localized site of bone formation appeared to be biphasic with a second elevation in expression at 4 days after delivery of the adBMP2 transduced cells (figure 17). This was not seen in the tissues receiving the Adempty transduced cells. We then quantified whether this led to new vessel formation, and found a 2 fold enhancement in new vessels in tissues receiving the BMP2 transduced cells (Fouletier-Dilling *et al,* 2010). We also demonstrated that cells expressing the VEGFs were the brown adipose (Fouletier-Dilling *et al,* 2010), and that the adipose appears to be generated rapidly, and involved in patterning of the newly forming bone. From these studies we have identified a novel mechanism which shows the molecular pathway induced directly by BMP2, which leads to production of brown adipose, new vessels, peripheral nerve ingrowth, and ultimately cartilage and bone (Olmsted-Davis *et al*, 2007).

d. *Test these gels in vivo. (Months 36-48)*

Please see previous sections (figure 10). We are currently testing the materials in rat models, through injection of the microspheres into the paraspinous musculature, similar to the rat studies, performed for the transduced cells. See page 22-23 of this report.

Task 3: To achieve posterolateral spine fusion by percutaneous injection of the encapsulated Ad5F35BMP2 transduced mesenchymal stem cells into the paraspinous musculature of both rats and mice. Spine fusion will be assessed in both a rat and mouse model by both histological and radiological analyses over time and confirmed by both microCT and biomechanical testing. The results will also be compared to a parallel murine system which is immunocompetent. These experiments will provide essential preclinical data in two different animal models.

a. Obtain approvals through the DOD institutional review board for approval to work with the human mesenchymal stem cells. **(Months 0-12)**

This was completed within the first few months of the award.

b. Once approved we will start to utilize these cells in all hydrogel formulation experiments as described in Task 2. **(Months 12-36)**

We chose to test the system in two different murine models: immune competent and immune compromised (Olabisi *et al*, 2011b). One major reason for testing both is that the proposed clinical system will utilize human mesenchymal stem cells transduced with an Ad5F35BMP2 vector for the production of BMP2 *in vivo* for spine fusion. Thus the immune compromised NOD/Scid mouse will allow us to test this system directly. However, we wished to demonstrate similar efficacy in a mouse model which is not immune compromised since presumably this system would be developed for the general population. Thus we also chose to test the system in C57BL/6 wild type mice, which require us to use a matched C57BL/6 derived cell line (MC3T3-E1).

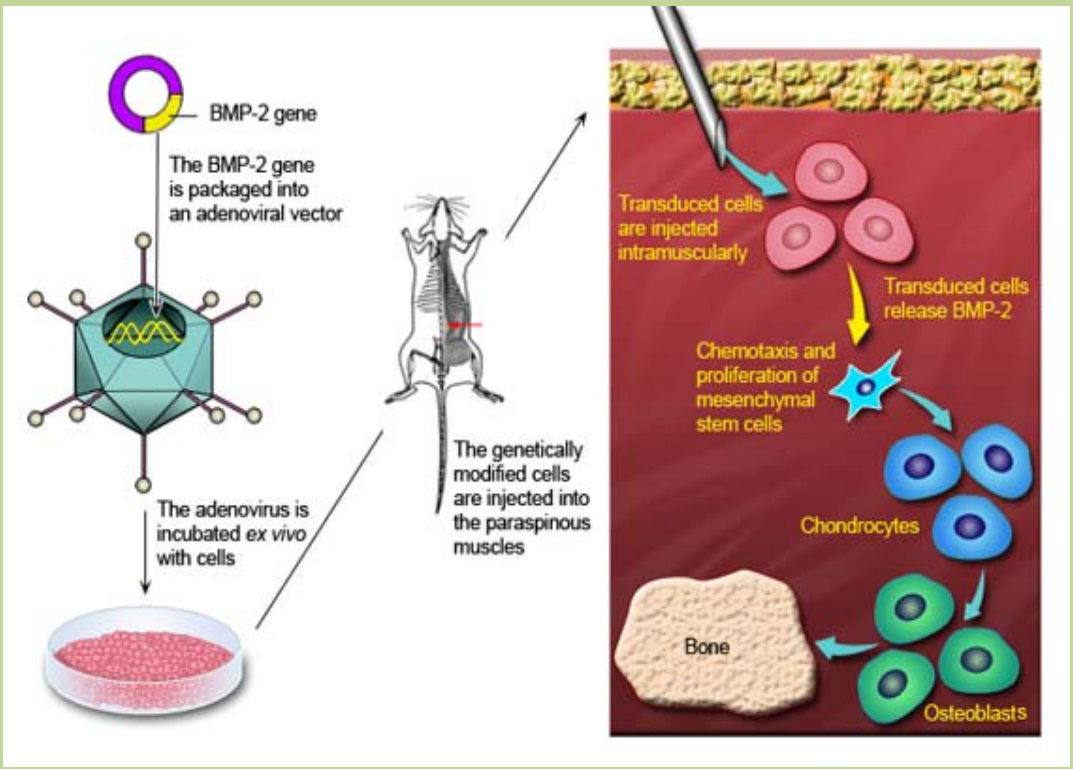

Figure 18: Schematic depiction of spine fusion using the cell based gene therapy system. AdBMP2 transduced cells injected into the muscle, rapidly recruit host cells to undergo all stages of endochondral ossification. Within one week mineralized osteoid can be detected in photomicrographs and radiographs.

The latter system also requires the inclusion of the polyamine compound gene jammer (Fouletier-Dilling et al, 2005). However, the gene jammer is not proposed to be a component of the final gene therapy system. Therefore we next tested the ability of the system to fusion multiple vertebra in both systems. For the NOD/Scid mice human fibroblasts, were directly transduced with an E1-E3 replication defective adenovirus vector which possesses a human BMP2 cDNA, in E1 and an altered fiber gene in which Ad5 fiber has been replaced with an Ad5F35 fiber, which we refer to as Ad5F35BMP2 vector (5000 vp/cell) whereas in the second model, MC3T3-E1 cells were transduced by addition of the gene jammer compound to the cells at time of infection with a standard E1-E3 deleted replication defective adenovirus type 5 vector possessing the same human BMP2 cDNA in E1, Ad5BMP2 virus (5000 vp/cell). Both systems routinely provide ≤90% transduction

efficiency (Fouletier-Dilling et al, 2005). Next 5 x 10^6 transduced cells were injected into the parapsinous musculature of the mice (n=10 Nod/Scid and n=3 C57BL/6). To insure proper placement the material was injected under anesthesia into the mouse, along the length of the paraspinous muscle in the lumbar spine adjacent to the desired fusion point, to allow the transduced cells to track the entire muscle region (Figure 18). The mice were then euthanized at various time points and the bone was analyzed by various criteria to ensure fusion. With this system, heterotopic ossification is generated rapidly, fused and remodeled into two or more of the adjacent vertebra, reducing spine motion.

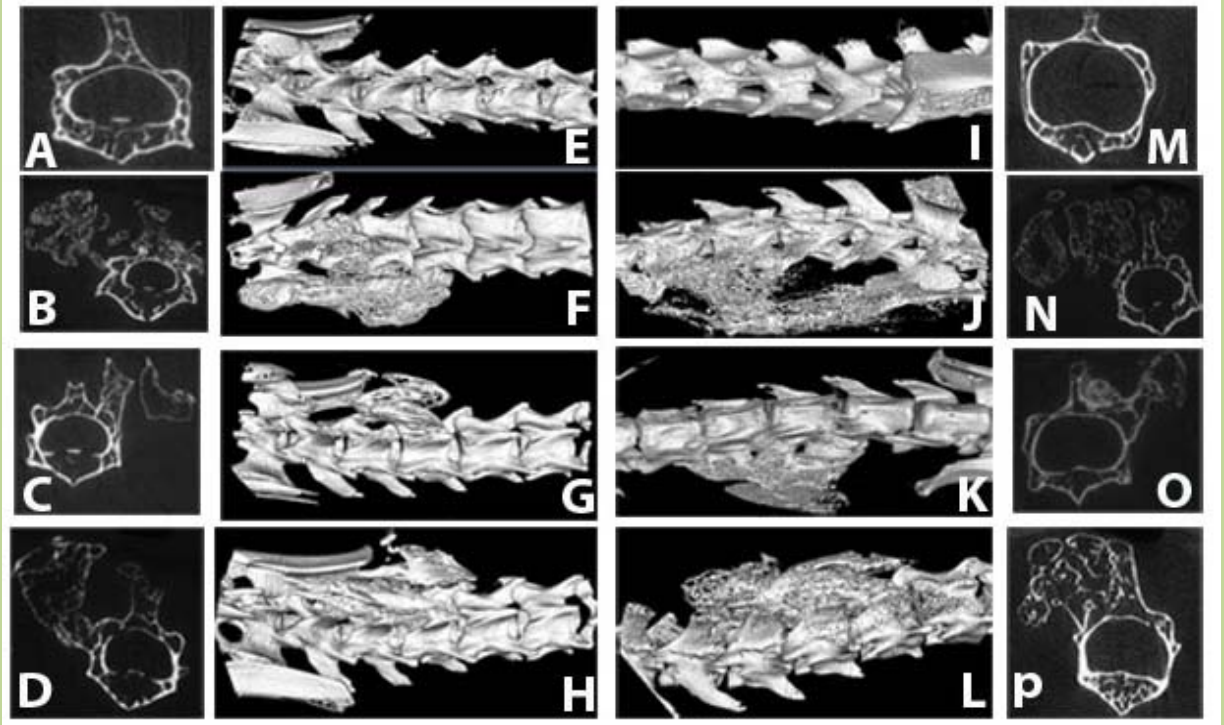

Figure 19: Radiographs of C57BL/6 (panels A-H) and NOD/Scid (panels I-P) spines imaged after intramuscular injection into the paraspinous musculature of cells transduced with Adempty cassette control virus (panels A, E, I, and M) or AdBMP2 (panels B-D, F-H, J-L, and N-P). Control animals injected with Ad5HM4 were scanned 6 weeks after delivery of the transduced cells (panels A, E, I and M). Mice receiving the AdBMP2 transduced cells, were scanned 2 weeks (panels B, F, J, N); 4 weeks (panels C, G, K, O); and 6 weeks (D, H, L, P) after the initial induction of heterotopic ossification. Two dimensional x-rays (panels A-D; C57BL/6 and panels M-P; NOD/Scid) show a cross section through the three dimensional reconstructions (panels E-H; C57BL/6 and I-L; NOD/Scid) of tentative fusions between the heterotopic ossification and the vertebral bone.

Radiological and microCT analysis of spine fusion: Accordingly heterotopic bone formation was allowed to progress for 2, 4 and 6 weeks, after initial injection of the AdBMP2 or empty cassette transduced cells. Spines were removed and analyzed for the presence of heterotopic bone, and spinal arthrodesis. In all AdBMP2 injections, heterotopic bone formation occurred along the injection site, adjacent to the spine, with greater than 90% bridging and fusing to the skeletal bone. (figure 19, three dimensional reconstructions E-L). Two dimensional radiographs (figure 19, panels A-D and M-P) show the cross sections through the tentative fusion. The radiographs and three dimensional reconstructions demonstrate that both the immune incompetent system, NOD/Scid mice receiving human cells transduced with AdBMP2 (panels I-P), and immune competent system, C57BL/6, receiving AdBMP2 transduced allogeneic murine cells (panels A-H); appear to produce similar bone within 4 to 6 weeks. This new bone appears to be remodeled with a contiguous cortical bone exterior. Although we did observe 40% of the samples in the NOD/Scid animals with potential points of fusion, panel N shows a scenario in which the heterotopic bone, although extensive, has not yet fused into the vertebrae. It appears in panel J, that the heterotopic bone occurred slightly distal to the vertebral bodies. Interestingly, we did not see similar findings in wild type mouse models, as seen in panel B even at two weeks the substantial bone has fused to the adjacent vertebra.

In the cross-sectional radiographs, vertebral cortical bone appears to be integrated with the heterotopic one (figure 19, panel B-D, O-P). The points of fusion appear to be in the laminae region of the vertebra, with the majority of cases encompassing the entire spinous and transverse processes, suggesting significant fusion. In this case although the location of the fusion is unchanged, only limited portions of the spinous and transverse process are actually integrated. In no case did we observe bone formation or bridging in the samples receiving the Adempty cassette transduced cells. The apparent fusion appeared to be rapid, within two weeks, and limited in size and scale, to region of muscle which received the cells. Further, at no time did we observe bone formation within the spinal canal.

To confirm that the apparent mineralized bone observed on the radiographs is true osteoid, and that it has integrated at these tentative points of fusion, we isolated the spine and adjacent tissues for histological analysis using techniques. The spines were embedded in paraffin blocks, five micron sections cut, and every fifth section was stained with hematoxylin and eosin to identify the tentative point of fusions. Representative photomicrographs (2X and 4X) of samples from either model, taken 2, 4 and 6 weeks after induction of heterotopic ossification are shown in figure 20. In all cases we observed structures of mature bone, such as osteoclasts, osteocytes and tentative bone marrow elements in the heterotopic bone, as well as cartilage, analogous to the growth plate structures in the normal long bone. However the heterotopic bone appeared to grow in a direction towards the skeletal bone, with the most mature bone being distal to the skeletal bone in the 2 week samples. Figure 20, panel A-B, shows that there is substantial new bone, adjacent and fused with the more mature vertebral bone, along the transverse process, and laminae region of the vertebra. Although mature bone with tentative marrow elements was observed at 2 weeks; this structure was always distal to the vertebral bone (data not shown), suggesting that the original heterotopic ossification started *de novo*, in the muscle and grew towards the vertebrae to encompass the bone. By four weeks, (figure 20, panel C-D), the heterotopic bone is much more mature, and at the point of fusion, a very cellular reaction, that appears to be rapidly removing the mature cortex of the skeletal bone was noted. It is unclear whether the large number of cells is recruited to this boundary or is expanding from the vertebral periosteum, but as noted in panel G, the mature cortical bone of the vertebra appears to be pitted and undergoing removal by the maturing heterotopic bone. By 6 weeks, this boundary is completely remodeled (figure 20; panel E-F) with the two bones now contiguous as one integrated structure with a well-defined cortex and trabecular interior, which houses the bone marrow. Interestingly, the only evidence remaining of the newly formed heterotopic ossification is the presence of substantial amounts of adipose tissue, which is found within heterotopic regions, in contrast to the mature marrow within the vertebra (panel F). Figure 20, all cases show what appears to be fusion with the transverse process within the laminae region of the vertebra, which was the target region for fusion. Depending on the depth of the section, more or less of this region was involved in the fusion site. In many cases the fusion actually encompassed both the spinous process through the laminae to the transverse process. In all tissues analyzed, the vertebral body did not appear to undergo growth, and there was no evidence of new bone formation within the spinal canal, similar to our observed radiological findings.

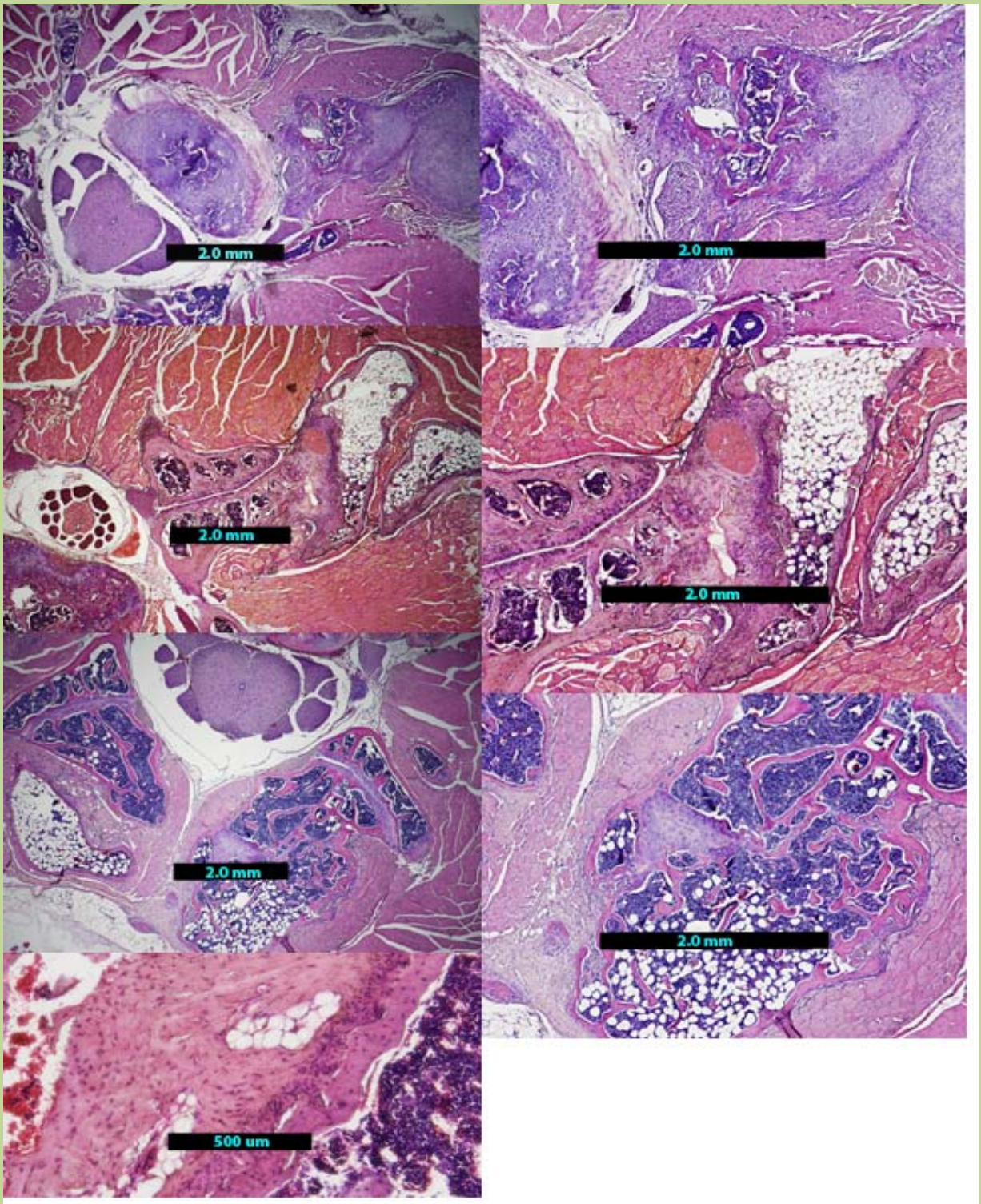

Figure 20: Representative photomicrographs of tentative vertebral fusion with the heterotopic bone, taken 2 (panels A-B; 2X and 4X respectively), 4 (panels C-D; 2X and 4X respectively), and 6 (panels E-F; 2X and 4X respectively) weeks after initial injection of the AdBMP2 transduced cells. The slides were stained with hematoxylin and eosin for viewing. Panel E is a representative photomicrograph (10X) of a sample taken 4 weeks after the initial injection of AdBMP2 transduced cells. As can be seen in this sample, there are a significant number of cells associated with the boundary between the new heterotopic and old vertebral bone.

The clinical goal of spine fusion is to reduce motion within the vertebral column; therefore, we developed a method for measuring flexion-extension of the spine. In this analysis spines were x-rayed before and after bending, and intervertebral motion was quantified using KIMAX QMA software (Medical Metrics, Inc.). This software has been validated to measure intervertebral motion with an accuracy of better than 0.5° of rotation and 0.5 mm of translation. Results of this analysis are shown in Table 1. In no cases did tissues receiving the Adempty cassette transduced cells, show a reduction in motion or spine stiffening. Whereas in NOD/Scid animals that received the human cells transduced with AdBMP2, approximately 40% of the spines at 2 weeks and 90% of those at 4 and 6 weeks had reduced movement, consistent with fusion of at least one level. Interestingly, the C57BL/6 group receiving AdBMP2 transduced cells, at all-time points, consistently showed a reduction in motion within the lumbar spine correlating with fusion (Table 1).

Table 1: Spinal fusion in injected animals

Group	N	Strain	Time	Spines with 2 or more vertebrae fused (%)
Adempty cassette transduced cells	9	NOD/Scid	6 weeks	0 %
AdBMP2 transduced cells	9	NOD/Scid	2 weeks	44 %
AdBMP2 transduced cells	9	NOD/Scid	4 weeks	90 %
AdBMP2 transduced cells	9	NOD/Scid	6 weeks	90 %
Adempty cassette transduced cells	8	C57BL/6	6 weeks	0%
AdBMP2 transduced cells	8	C57BL/6	2 weeks	100%
AdBMP2 transduced cells	4	C57BL/6	4 weeks	100%
AdBMP2 transduced cells	8	C57BL/6	6 weeks	100%

To further confirm spine fusion, the isolated spines used for mechanical testing were bleached to remove soft tissues, and analyzed on a gross level to see if the bone was contiguous. Figure 21, panel A, a representative 6 week spine shows that in this fusion, 5 vertebrae of the lumbar spine are actually remodeled into a single structure. In all cases with biomechanical constraint of the spine after the induction of bone formation, there was also integration of the vertebra with heterotopic bone, which was observed after removal of the soft tissues. In cases that did not meet our criteria for fusion (several NOD/Scid animals at 2 weeks) in that they did not appear to be constrained after induction of bone formation, there was heterotopic bone that was not integrated with the vertebrae but rather individual bones, confirming our biomechanical findings.

Further, in both immune competent and incompetent models the radio-micrographs show a distinct scoliosis in 6 month old growing mice, which received the Ad5BMP2 transduced cells injected into one side of the paraspinous musculature that parallels the spine. Figure 21, panel C, representative radiographs show a distinct curvature of the spine towards the area of new bone formation and tentative fusion. This was observed in a large number of animals with heterotopic bone and tentative fusion, but absent in animals that received the control cells (panel B). Within 4 weeks we observed 100% fusion in all the spines, and between 30-100% in just 2 weeks after injection of the material.

We next attempted to repeat this process in the using the microbeads. Figure 22A shows the resultant new bone formation between the transverse processes of the spine, after injection of the osteoinductive microspheres. The microspheres appear to retain the bone formation to immediately surrounding the polymer and in this case we have attempted to fuse three levels of the spine. As was the case with the directly injected cells, the spine was stabilized in approximately two weeks. The stippled pattern of the bone on x-ray represents the non-degradable version of the microspheres within the newly forming bone. Histologically as shown in the figure 16 the bone is of normal structure. In all cases when the Adempty cassette transduced

cells micro-encapsulated in the PEGDA hydrogel were injected between the transverse processes, the no new bone formation was observed. The PEGDA material is not radio-opague and therefore cannot be visualized through x-ray. Therefore in these studies the microspheres appeared to work as reliably at fusing the spine as the cells when directly injected.

Figure 21: Spine fusion was observed in bones isolated from the mouse after induction of targeted heterotopic ossification (panel A). Associated soft tissues were removed by bleaching, leaving only the bone. A wire was threaded through the spinal column, to preserve the orientation of the vertebra. Unfused vertebrae hang free; fused vertebrae remain joined and rigid. Ruler is in millimeters. Radiographs of mouse spines 6 weeks after induction of spine fusion Adempty cassette (panel B) or AdBMP2 (panel C) transduced cells. Panel C, shows obvious curvature of the spine suggesting a significant scoliosis, as compared to the normal mouse spine, shown in panel B.

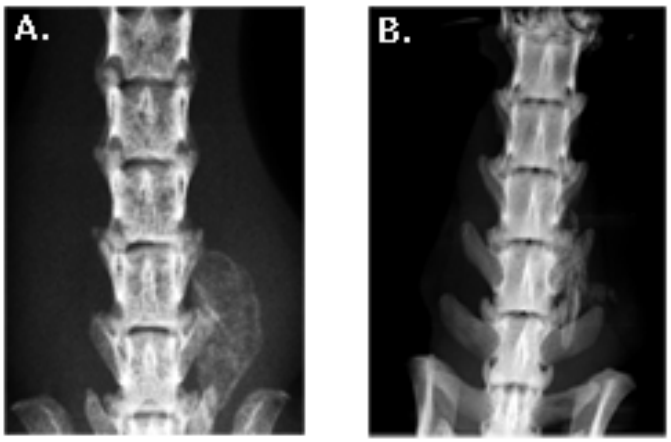

Figure 22: X-ray of a mouse (A) and rat (B) spines after a injected with AdBMP2 transduced cells micro-encapsulated in PEGDA hydrogel microspheres. This is a representative x-ray of 5 animals. In all cases the animals receiveing the Adempty cassette transduced cells encapsulated in the hydrogel, did not result in any bone formation.

Because we next wanted to determine if we could translate our findings in mice into a wild type outbred rat strain, we next injected a serious of Wistar rats with microspheres encapsulating AdBMP2 or Adempty cassette transduced wistar rat skin fibroblasts into the hind limb musculature to ensure that we could rapidly induce heterotopic ossification (HO) (n=10 rats in all experiments). Results of this study are shown in figure 23. Surprisingly, when the microspheres were injected proximal to the skeletal bone, rapid bone formed, but when the microspheres were placed more distal, we observed no bone formation. We hypothesized that BMP2 may be able to extent outward from the microspheres in a gradient, which when close to skeletal bone, could mobilize progenitors, but when embedded in muscle more distal from the skeleton was unable to induce HO. Therefore we next attempted to rescue bone formation by add human mesenchymal stem cells. These cells have previously been shown to incorporate into bone and function as osteoblast progenitors. As seen in figure 23, no bone formation was observed in rats (n=10) when microspheres were injected in combination with the MSCs. Previous studies in the laboratory have demonstrated the role of peripheral nerves in the induction of heterotopic ossification. In a separate project we have isolated a cell within the perineurial-endoneurial regions of peripheral nerves that is essential for heterotopic bone formation. In its absence BMP2 induction does not work. Therefore, we next attempted to rescue bone formation by including cells isolated by collagenase digestion from rat sciatic nerve with the osteoinductive microspheres. As seen in figure 23, heterotopic ossification was not only rescued but appeared to be as robust as when near the skeletal bone. Interestingly, it is well known that peripheral nerves are

surrounded by an organized collagen matrix known as the epineurium, which prevents agents from the exterior of the nerve from entering the peri-and endoneurium. In order to regulate peripheral nerve-axonal function, extremely high levels of drugs must be delivered in order for a small amount to enter through the matrix.

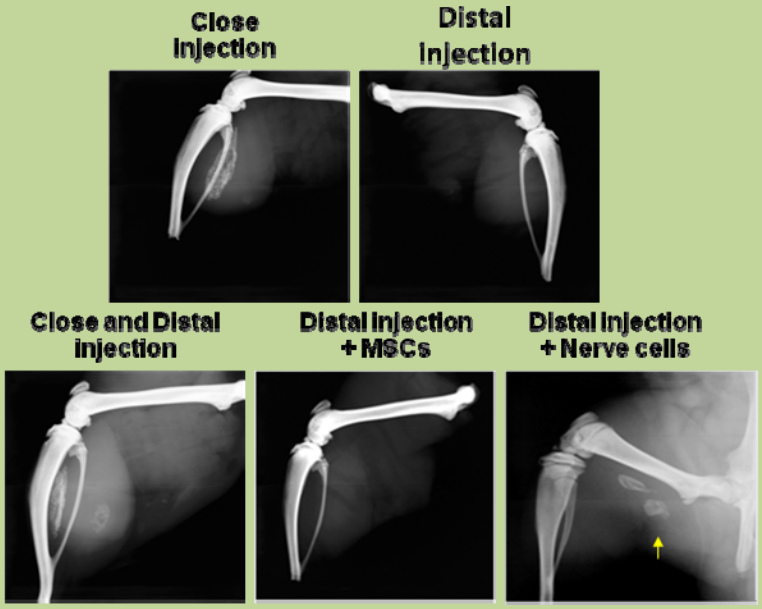

Figure 23: Radiographic analysis of heterotopic bone formation in wild type rats. Injection of the osteoinductive microspheres at varying locations with respect to skeletal bone with no additions or inclusion of primary human mesenchymal stem cells or the cellular component of sciatic nerves.

Alternatively this matrix must be degraded. Thus, it may not be surprising that high levels of BMP2 have been required in order to induce bone formation. Most likely this is due to the requirement for BMP2 to induce both remodeling of the epineurium, and to access the peri- and endoneurial cells required for bone formation. **The results of these studies suggest that elevated physiological levels of BMP2, may be quite effective in rapidly induce bone repair and restoration of the soft tissues.** In support of this idea, the human genetic disorder Fibrodysplasia ossificans progressiva (FOP), that has a constitutively active BMP receptor, requires specific soft tissue injuries in order for heterotopic bone to form, supporting our finding that elevated physiological levels of BMP2 can reliably and rapidly restore bone formation when these unique nerve stem cells are present.

We next tested the ability to induce bone formation using the microspheres for spine fusion. Rats were injected with microspheres encapsulating either Ad5BMP2 or Adempty cassette transduced cells and two weeks later bone formation assessed by x-ray and subsequent histological analysis. The shadowing around the spine in figure 24A was confirmed to be bone through histological analysis, although there was also a substantial amount of cartilage as seen in figure 24C and D. This data collectively suggests that our osteoinductive microspheres possess the potential to reliable fuse the spine after injection.

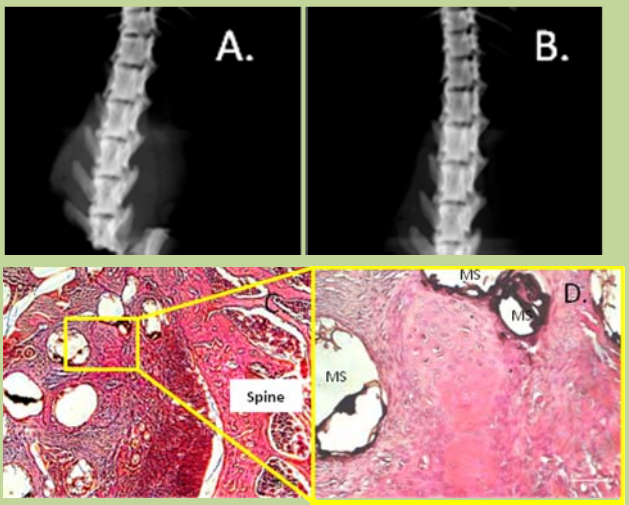

Figure 24: Analysis of new bone formation and spine fusion in a Wistar rat model. Wistar rat skin fibroblasts (2 x 10e7 cells) were transduced with (A.) Ad5BMP2 (B.) Ad5empty cassette

c. Once the gels have been modified to offer optimal properties for bone formation and removal, we will test these in a murine model of spine fusion. **(24-36 months) These studies are ongoing in the rat model since it is more challenging.**

d. Since we have substantial knowledge of the mouse model, we will initially start to collect data with this system. We will demonstrate the ability to induce spine fusion in the presence of tetracycline. **(Months 24-40)** We most likely will not attempt these, since we have an alternative method for looking at gene expression that may be more effective at removing the cells, and transgene expression. Tetracycline vectors are already established but these types of safety switches have been obsoleted by the inducible caspase systems. We have established this system and demonstrated in vitro, that the cells will undergo apoptosis in the hydrogel micropsheres in the presence of the dimerizing compound. Additionally, we have some preliminary data in the mouse that suggests that we can selectively remove the

AdBMP2 transduced cells by delivery of the specific agent that activates the caspase and subsequently program cell death in the transduced cells.

e. Analyze the modified injectable hydrogel for optimal volume, *in vivo* crosslinking, design, selective degradation, and inflammatory reaction using both live animal imaging and histology. **(Months 24-48)**

We will no longer be crosslinking *in vivo* since we are actually attempting to perform the specific microbead structures for optimal cell viability and BMP2 secretion. These structures are actually injectable, and thus will be utilized similarly to the direct injection of the cells. Preliminary data suggests that these structures will provide for even more rapid and reliable fusion of the spine. In this next phase of the grant, we will be encapsulating human mesenchymal stem cells that possess a caspase gene, which will provide a method for timed cell removal. In this case we will add the activator of caspase to send the BMP2 transduced cells through apoptosis, paralleling the timing of remodeling of the PEG-DA hydrogel microbead structures. Thus we will ensure that we destroy the cells within the PEG-DA hydrogel microbead structures, prior to potential degradation of the polymer. These studies with the human mesenchymal stem cells will also be tested using the IFP4.1 reporter so that we can track their viability in the presence of the drug, as well as determine the optimal timing of BMP2 secretion for bone formation. This is actually the final phase of the proposed set of studies, and should allow us to arrive at a final product for testing.

f. All fusions will be tested both biomechanically as well as radiologically using microCT to confirm the fusion. **(Months 40-48)**

This aim is complete! A method to reliably determine if newly mineralized tissue adjacent to the spine has formed a structurally competent bridge between vertebrae is needed to assess new spine fusion technologies in small animal models. Micro-computed tomography can be used to visualize any newly formed mineralized tissue adjacent to the spine, but it can be difficult in some cases to determine if the mineralized tissue is actually integrated with the vertebrae or if it is only overlying the vertebrae. Micro-CT exams also require expensive equipment and long-scan and post-processing times. To provide a simple and rapid method to directly test whether a fusion was mechanically successful, a mechanical device was developed that creates controlled flexion and extension in a mouse spine, so that spine fusions could be assessed using the same computer-assisted methods that are now widely used to assess spine fusions in human patients. This device was validated in a mouse spine fusion model. Utilization of the device involves embedding the spine and surrounding tissues, after removal from the body, in mold using rapid setting alginate. The embedded spine is then flexed using the device and a micro-radiograph is obtained with a digital Faxitron system. The embedded spine is then placed in extension and a second radiograph is obtained. These two radiographs are then imported into a workstation and analyzed using previously validated computer-assisted technology (Zhao KD, *et al*.2005). The software allows intervertebral motion to be accurately quantified. A successful spine fusion is intended to stop any significant motion between vertebrae. In the human spine, intervertebral motion under 1.5 degrees at any level is considered to be reliable evidence of a solid spine fusion (Hipp JA et al, 2008) using this image processing technology.

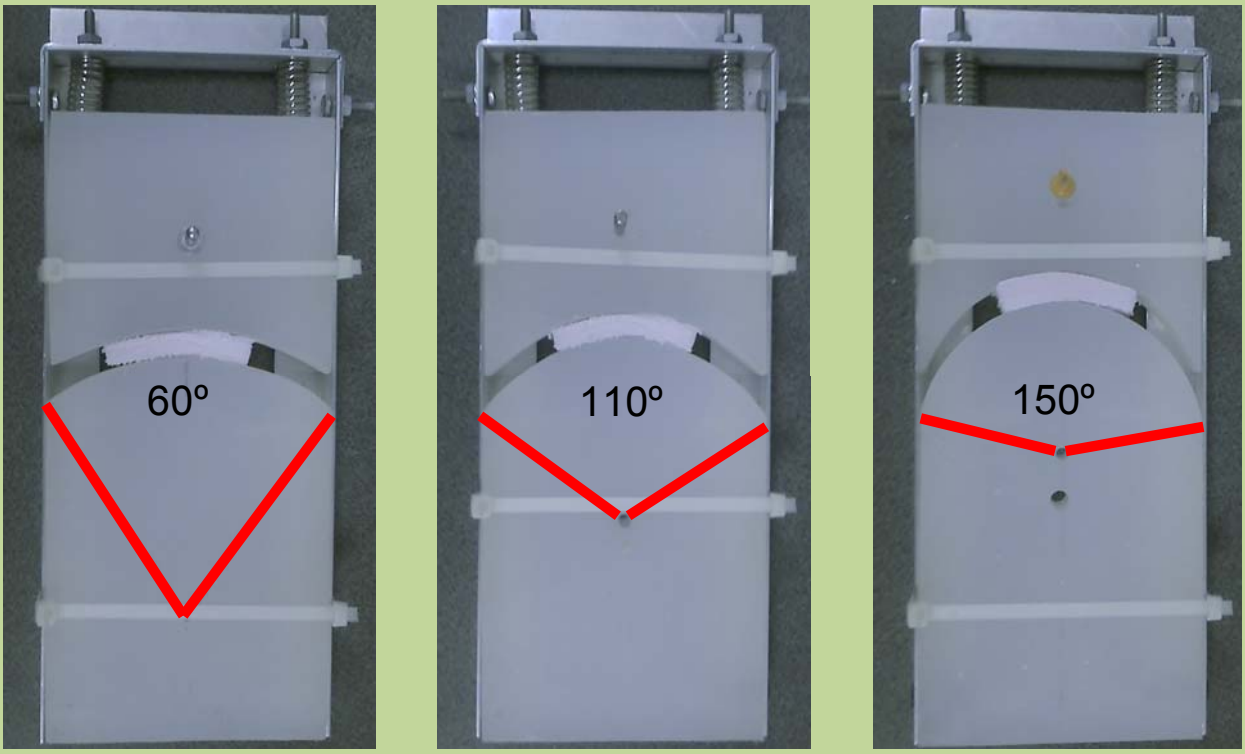

Figure 24: Angles and apparatus to flex and extend the spines after fusion, to determine if the degree of motion has been restricted in the murine model, to a similar extent to what would need to be achieved to reduce pain in a human clinical setting.

To test whether the tentative fusions were actually capable of reducing motion within the spine, we set up some experiments to look at flexion/tension under bending at specific angles. Briefly, three groups of NOD/Scid mice were given an injection of MRC5 cells transduced with 1) Ad5F35BMP2 (2 week analysis), 2) Ad5F35BMP2 (6 weeks), and 3) Ad5F35empty cassette all at 2500 vp/cell. The cells were transplanted into the paraspinous musculature of through direct injection. Group 1 animals were isolated at 2 weeks, while groups 2 and 3 were harvested at 6 weeks after initial induction. The spines were then embedded in an agarose gel material, and placed between two plates for bending analysis (figure 26).

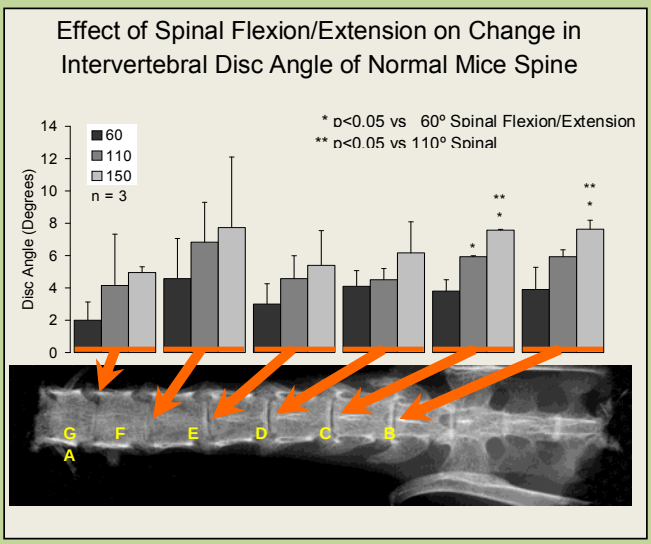

Figure 25: Results of analysis of the disc angle after bending at 60,110, and 150 degree angles. Each column of numbers represents the corresponding disc (arrow). The results suggest more variability in discs on the end of the animal, where the spine has been cut, versus internal or adjacent to the pelvis which remains on these tissues.

To determine what to expect for normal spine flexibility in these mice, we subjected a group which had received no treatment to this analysis. As can be seen in figure 23, the values obtained from subjecting the mice to 60°, 110°, and 150° angle varied significantly at the ends of the spine and most likely due to the isolation, and the fact that the spine had been cut. Discs within the center and lower spine showed significance between 60 and 110 degree shifting with little or no variability, and allowed us to focus on this region for analyzing our fusions (figure 26). This technique has been published (Dewan *et al*, 2011).

g. Once we have established methodology that leads to reproducible fusion we will further test this in a rat model of spine fusion using athymic rat's spine fusion using athymic rats. We will then compare and confirm that these results are similar to those obtained in immuno-competent mice. **(Months 40-48)**

We have extensively compared the production of BMP2 and resultant bone formation in immune competent and incompetent mice (Fouletier- Dilling et al, 2007), and have found there to be no difference between the two systems, as long as the BMP2 expression remained equivalent. We have further confirmed this to be true for the material after hydrogel encapsulation, including when delivered to rats. Thus we have focused predominantly on obaining bone formation and spine fusion in the wild type animals (figure 23). As noted, we have finishing experiments in rats, which appear to confirm our findings in mice, where AdBMP2 or empty cassette transduced cells were directly injected into the paraspinous musculature for posterior lateral spine fusion. This completed 90% of the grant application. The remaining experiments are to demonstrate the ability to remove the polymer after bone formation as occurred through bone remodeling, thus restoring the bone to its native structure and eliminating any foreign materials. We hope to focus on completing these experiments during the no cost extension period of this project.

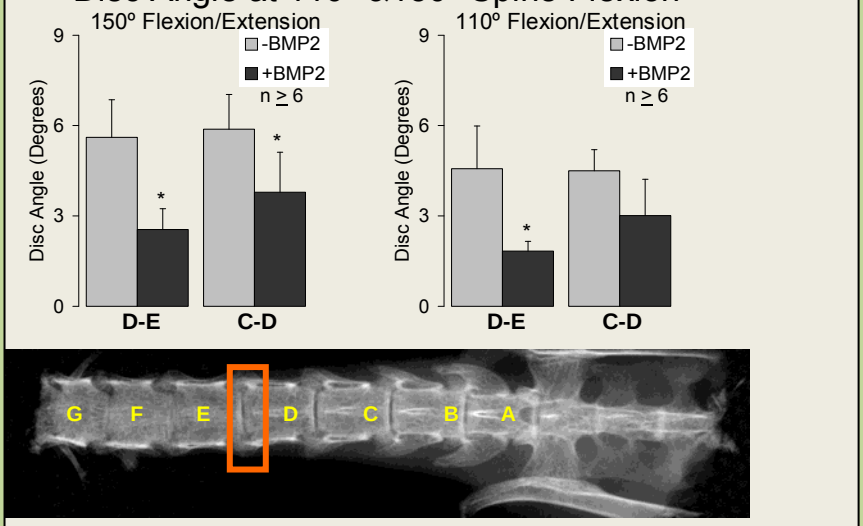

Figure 26: Results of analysis of the disc angle after bending at110, and 150 degree angles in tissues isolated from mice 6 weeks after induction with BMP2. The disc analyzed is listed as the disc between the two lettered vertebras. The disc which provided the most significance in limiting the disc angle is highlighted by the orange box. This sample is representative of the group of fused spines.

h. To initiate toxicology studies, as potentially outlined in a pre-IND meeting with the FDA. **(Months 24-48)**

We have been focused on completing efficacy as described above, and now have obtained a final formulation that can readily be manufactured. To this end, we have focused on cryopreservation, of microbeads-AdBMP2 transduced cells, to complete the the formulation. In these studies we propose to freeze the encapsulated cells in a ready-to-go formulation that could be thawed just prior to the procedure, washed gently with PBS, and immediately loaded into a syringe. If successful, batches of the materials could be generated and frozen as a bank for clinical implementation. We propose that the materials could be shipped to hospitals, or outpatient clinics, and then through image guided paraspinous injections. This would not require surgery, and would be able to be implemented through non-invasive injections. The patient could resume their normal activity, and fusion be confirmed through standard clinical means, at 2 and 4 weeks after injections. To confirm that the materials could survive cryopreservation we next transduced cells with adenovirus, and cryopreserved a portion of them, and then thawed, and plated to compare to the normal cells. Morphologically the cells appear normal after freezing; we next looked at cell viability after microencapsulation of the cells, both before and after freezing. As seen in figure 27, the cell viability appears to be similar between these populations, with dead cells (red-dsRED) being much lower, than the live (green – GFP) in both cases. We are currently measuring the level of BMP2 expression from frozen and non-frozen AdBMP2 transduced cells, encapsulated in microspheres, to determine the effects of freezing on transgene expression. However, we predict that it is highly unlikely to have changed, since the cell viability remains similar. After confirmation of the BMP2 level of expression, we will also inject the thawed microspheres into the animal and confirm heterotopic bone formation. We will analyze the tissues to ensure there are no apparent changes in the bone formation, or inflammatory responses due to the freezing process.

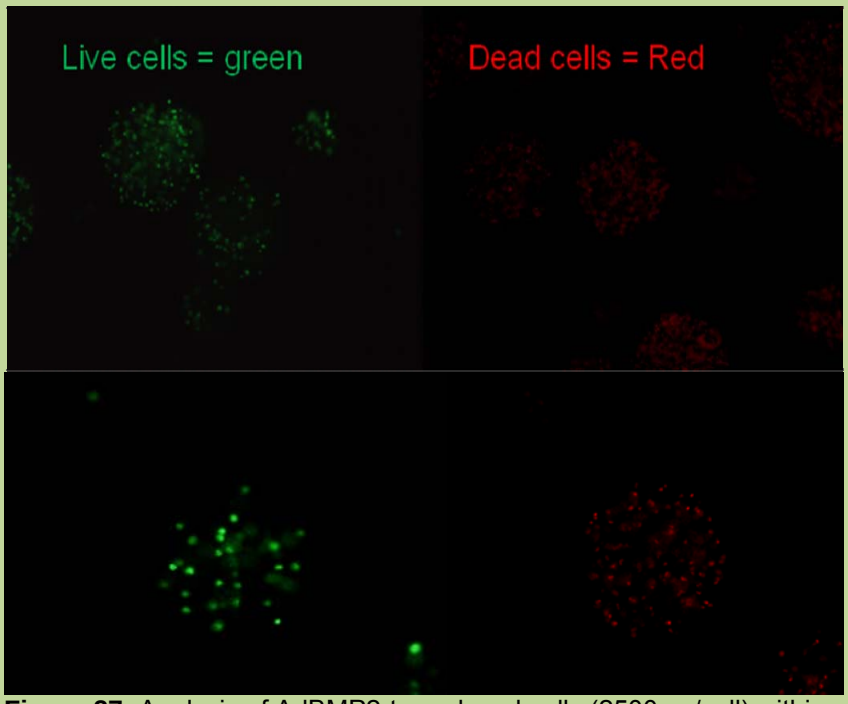

Figure 27: Analysis of AdBMP2-transduced cells (2500 vp/cell) within microspheres was assessed at day 7 using a LIVE/DEAD® Viability/Cytotoxicity Kit for mammalian cells (Invitrogen, Molecular Probes, Eugene, OR). Panel A and B show the cells within the microspheres after freezing, and panels C and D prior to freezing. Live cells are indicated by green and dead cells by red. Our preliminary quantification of the cells suggests that there are similar numbers of live and dead cells before and after freezing.

Key Research Accomplishments

- We have developed a method for monitoring BMP2 expression in live animals through the use of dsRED. This optical imaging modality appears to be specific and significantly more sensitive than either lucerifase imaging or GFP detection. We have initiated studies to look at the regulated BMP2 carrying a dsRED gene and compare bone formation in the presence of long term versus short term BMP2 expression. *Olabisi RM, et al., Tissue Eng Part A. 2010 Dec;16(12):3727-36.*
- We have developed a formulation of hydrogel that provides for sufficient BMP2 expression to induce *in vivo* bone formation. We have shown that these novel microbead structures efficiently secrete functional BMP2 and can produce heterotopic bone in the mouse hindlimb. The cells encapsulated in these structures survive a significantly longer time period than their directly injected counterparts, and they make significantly more bone than any of the other PEG-DA hydrogel structures tested. These are easily injected and appear to reside at the injected location. *Olabisi RM, et al., Tissue Eng Part A. 2010 Dec;16(12):3727-36.*
- We have demonstrated that introduction of osteoclast degradation sites within this material provide selective degradation by osteoclasts similar to skeletal bone remodeling. We have synthesized the peptide sites and introduced them into the PEG-DA strands and succeeded in getting normal crosslinking of the material. We have then degraded the hydrogel completely in the presence of either a general protease (proteinase K) or a specific proteinase (cathespin K) but not with other selective proteinases. We have shown that both osteoblasts and osteoclasts can attach to the material, but only osteoclasts can lead to its degradation. We have initiated *in vivo* testing and found that the microbeads are degrading slowly, and appear to be replaced with mature bone. *Hsu CW, Olabisi RM, Olmsted-Davis EA, Davis AR, West JL. J Biomed Mater Res A. 2011 Jul;98(1):53-62. Epub 2011 Apr 26*
- We have recently developed a method for confirming spine fusion through flexion and extension measurements. This is a critical component to characterizing the biomaterial, since on many occasions' microCT or x-ray analysis can appear as a true fusion, however, upon bending the heterotopic bone will break at the fusion site rather than constrain the spine, as a result of poor fusion, and remodeling with the normal skeletal bone. This work has allowed us to confirm that spine fusions as denoted by radiological or histological approaches are also capable of restraining motion in the spine, the clinical gold standard of spine fusion. *Dewan AK, Dewan RA, Calderon N, Fuentes A, Lazard Z, Davis AR, Heggeness M, Hipp JA, Olmsted-Davis EA. J Orthop Surg Res. 2010 Aug 21;5:58.*
- We have completed testing spine fusion in the mice using large groups, to ensure we have a valid sample size. The first groups used for this experimental design for direct injected cells and confirmed spine fusion within 4 weeks. *Olabisi RM, Lazard Z, Heggeness MH, Moran KM, Hipp JA, Dewan AK, Davis AR, West JL, Olmsted-Davis EA. Spine J. 2011 Feb 1*
- We are currently now testing tentative spine fusions in both wild type mice and rats receiving the hydrogel encapsulated cells. We should complete this work in approximately 3 months.
- We are currently demonstrating the ability to cryopreserve the AdBMP2 transduced cells which have been encapsulated into the microspheres, and completing efficacy testing in rats with our final product. *This work has been submitted for publication in Cells and Biomaterials for Tissue Repair, special issue.*
- We have current submitted a provisional patent application on this material.
  International Patent Application No.: PCT/US2010/58603
  Title: Methods and Compositions for Bone Formation
  Filling Date: December 1, 2010
  Inventor: Elizabeth A. Davis, et. al.

Reportable Outcomes:

Oral presentation:

Ronke M. Olabisi, Chi-Wei Hsu, Alan R. Davis, Elizabeth A. Olmsted-Davis, Jennifer L. West. Cathepsin-K Sensitive Poly(ethylene) Glycol Hydrogels for Degradation in Response to Bone Formation. In Society for Biomaterials Annual Meeting and Exposition, San Antonio, TX, April 22 – 25, 2009.

Ronke M. Olabisi, Chi-Wei Hsu, Alan R. Davis, Elizabeth A. Olmsted-Davis, Jennifer L. West, Cathepsin K Sensitive Poly(ethylene) Glycol Hydrogels for Degradation in Response to Bone Formation. In Gordon

Research Conferences – Biomaterials: Biocompatibility/Tissue Engineering, Holderness, NH July 19 – 24, 2009.
Sonnet C, Rodenberg EJ, Salisbury EA, Olmsted-Davis EA, Davis AR. A model for neuronal regulation of heterotopic ossification. Conference: 7th International Society of Musculoskeletal and Neuronal Interactions (ISMNI). Cologne, Germany, May 2010. Presenter - Corinne Sonnet.

Olmsted-Davis E. A., Davis, A.R. and West, J. L. The Role of the Peripheral Nervous System in Heterotopic Ossification. Advances in Mineral Metabolism and John Haddad Young Investigators Meeting/ASBMR, Aspen, CO April 6-10.

Ronke M. Olabisi, ZaWaunyka Lazard, Mary Hall, Eva Sevick, Alan R. Davis, Elizabeth A. Olmsted- Davis, Jennifer L. West, Hydrogel microspheres increase cell survival and increase new bone volume in a gene therapy bone formation model. In Society for Biomaterials Annual Meeting and Exposition, Seattle, WA, April 21 – 24, 2010.

Ronke Olabisi, Corinne Sonnet, ZaWaunyka Lazard, Chartrisa Simpson, Alan Davis, Jennifer West, Elizabeth Olmsted-Davis, Hydrogel Microencapslation Permits Critical Size Defect Repair Via Gene Therapy. In Society For Biomaterials Annual Meeting and Exposition, Orlando, FL April 13-16, 2011

Ronke M Olabisi, Corinne Sonnet, C LaShan Simpson, ZaWaunyka Lazard, Kayleigh Sullivan, Alan R Davis, Jennifer L West, Elizabeth A Olmsted-Davis, Robust Femoral Critical Size Defect Repair via Injection of Hydrogel Microencapsulated Transduced Allogeneic Cells, The Gordon Research Conferences: Biomaterials & Tissue Engineering, Holderness, NH, Jul , 31 – August 5, 2011.

Olmsted-Davis, et al. Osteoinductive microspheres. Bone Disease Program of Texas, Houston, TX March 2nd, 2011.

Poster presentation:
Z Lazard, R Olabisi, A.R. Davis, J. West, and E Olmsted-Davis. An injectable Method for Spinal Fusion. Texas Bone Program Annual Meeting, May 10, 2010. Houston TX.

E. Salisbury, Z. Lazard, E. Rodenberg, A.R. Davis, and E.A. Olmsted-Davis. Neuronal Regulation of Early Heterotopic Ossification. Texas Bone Program Annual Meeting, May 10, 2010. Houston TX.

Ronke M. Olabisi, Chi-Wei Hsu, Alan R. Davis, Elizabeth A. Olmsted-Davis, Jennifer L. West, Cathepsin-K and Osteoclast Sensitive Poly(ethylene) Glycol Hydrogels. In 56th Annual Meeting of the Orthopaedic Research Society, New Orleans, LA, March 6 – 10, 2010.

Ankit Rajgariah, Ronke Olabisi, Ph. D., Lashan Simpson, Corrine Sonnet, Alan R. Davis, Elizabeth Olmsted-Davis, Jennifer West, Determining The Number of Cells Encapsulated When Making PEG-DA Hydrogel Microspheres. In Biomedical Engineering Society Annual Meeting, Austin, TX Oct 6-9, 2010.

Ronke M Olabisi, ZaWaunyka Lazard, Mary Hall, Eva Sevick, Alan R Davis, Elizabeth A Olmsted-Davis, Jennifer L West, Hydrogel microspheres increase cell survival and increase new bone volume in a gene therapy bone formation model. In Society for Biomaterials Annual Meeting and Exposition, Seattle, WA, April 21 – 24, 2010.

Jennifer Mumaw, Erin Jordan, Corinne Sonnet, Ronke Olabisi, Elizabeth Davis, Alan Davis, Jennifer West, Steven Stice. Cryopreservation of encapsulated therapeutic cells in a model for bone regeneration. Petit Institute for Bioengineering and Bioscience Industrial Partners Symposium. Atlanta, GA Oct 21-22, 2010.

Ronke Olabisi, Corinne Sonnet, ZaWaunyka Lazard, Chartrisa Simpson, Alan Davis, Jennifer West, Elizabeth Olmsted-Davis, Critical Size Defect Repair through a Single Injection. In 57th Annual Meeting of the Orthopaedic Research Society, Long Beach, CA, January 13-16, 2011.

Sonnet C, Olabisi R, Sullivan K, LaShan Simpson C, Hipp J, Davis AR, West JL, and Olmsted-Davis EA. Induction of heterotopic ossification in rats requires skeletal bone. Bone Disease Program of Texas, Houston TX. May 6, 2011 (Award winner for best project).

Corinne Sonnet Ph.D., Ronke Olabisi Ph.D., Kayleigh Sullivan, LaShan Simpson Ph.D., John Hipp Ph.D., ZaWaunyka Lazard, Zbigniew Gugala M.D., Ph.D., Francis Gannon M.D., Steve Stice Ph.D, John Peroni DMV, Michael Weh DMV, Eva Sevick Ph.D, Michael Heggeness M.D., Ph.D., Alan R. Davis Ph.D., Jennifer West Ph.D. and Elizabeth Olmsted-Davis Ph.D. Cell based gene therapy for fracture healing on a rat femural critical size defect. American society for Bone and Mineral Research Annual Meeting San Diego, CA Sept 16-17, 2011.

Manuscripts:

1. Dilling CF, Wada A, Lazard Z, Salisbury E, Gannon F, Vadakkan T, Gao L, Hirschi K, Dickinson M, Davis AR, Olmsted-Davis E. (2009) Vessel Formation is Induced Prior to the Appearance of Cartilage in BMP2-Mediated Heterotopic Ossification. J Bone Miner Res. J Bone Miner Res. 2010 May;25(5):1147-56. PMID: 19839764
2. Ronke M. Olabisi, Zawaunyka Lazard, Mary Hall, Eva Sevick, John A Hipp, Alan R. Davis, Elizabeth A. Olmsted-Davis and Jennifer L. West. Hydrogel microsphere encapuslation of a cell based gene therapy system, increases cell survival, transgene expression, and bone volume in a model of heterotopic ossification. Tissue Eng Part A. 2010 Dec;16(12):3727-36. Epub 2010 Sep 1.PMID: 20673027
3. Ashvin K. Dewan, Rahul A. Dewan, Nathan Calderone, Angie Fuentes, ZaWaunyka Lazard, Alan R. Davis, Michael H. Heggeness, John A. Hipp, and Elizabeth A. Olmsted-Davis. Assessing Mechanical Integrity of Spinal Fusion by *in situ* Endochondral Osteoinduction in a Murine Modal J Orthop Surg Res. 2010 Aug 21;5:58. PMID: 20727195
4. Ronke M Olabisi, Zawaunyka Lazard, Michael Heggeness, Kevin M Moran, John A Hipp, Ashvin Dewan, Alan R. Davis, Jennifer L. West and Elizabeth A. Olmsted-Davis. An Injectable Method for Spine Fusion. Spine J. 2011 Feb 1. [Epub ahead of print] PMID: 21292563
5. Chih-Wei Hsu, Ronke M. Olabisi, Alan R. Davis, Elizabeth A. Olmsted-Davis, Jennifer L. West . Cathepsin-K sensitive poly(ethylene Glycol) hydrogels for degradation in response to bone formation. J Biomed Mater Res A. 2011 Apr 26. [Epub ahead of print] PMID: 21523904
6. Elizabeth Salisbury, B.S., Corinne Sonnet, Ph.D., Michael Heggeness, M.D., Alan R. Davis, Ph.D., Elizabeth Olmsted-Davis, Ph.D. Heterotopic Ossification has Some Nerve Crit Rev Eukaryot Gene Expr. 2010;20(4):313-24. Review. PMID:21395504.
7. Z. Lazard, M. Heggeness, R. M. Olabisi, C. Hsu, J.A. Hipp, F. Gannon, A. R. Davis, J. L. West, and E. Olmsted-Davis. Cell Based Gene Therapy for Repair of Critical Size Defects in the Rat Fibula. J Cell Biochem. 2011 Jun;112(6):1563-71. [Epub ahead of print.] PMID:2134448.
8. A. Azhdarinia, N. Wilganowski, H. Robinson, P. Ghosh, S. Kwon, A.R. Davis, E. Olmsted-Davis, and E.M. Sevick-Muraca. Characterization of chemical, radiochemical and optical properties of a dual-labeled MMP-9 targeting peptide. Bioorg Med Chem. 2011 Jun 15;19(12):3769-76. Epub 2011 May 6. PMID:21612930.
9. Elizabeth Salisbury, Eric Rodenberg, Corinne Sonnet, Francis Gannon, H. David Shine,Tegy Vadakkan, Mary Dickinson, Elizabeth A. Olmsted-Davis, and Alan R. Davis. Sensory Nerve Induced Inflammation Contributes to Heterotopic Ossification. J Cell Biochem. 2011 Jun 15. doi: 10.1002/jcb.23225. [Epub ahead of print] PMID:21678472.
10. Eric Rodenberg, ZaWaunyka Lazard, Ali Azhdarinia, Mary Hall, Sunkuk Kwon, Nathaniel Wilganowski, Maria Merched-Sauvage, Elizabeth A. Salisbury, Alan R. Davis, Eva Sevick-Muraca, and Elizabeth Olmsted-Davis. Matrix Metalloproteinase-9 is a Diagnostic Marker of Heterotopic Ossification in a Murine Model. Tissue Eng Part A. 2011 Aug 2.
11. Mumaw J, Jordan ET, Sonnet C, Olabisi RM, Olmsted-Davis EA, Davis AR, Peroni JF, West JL, West F, Lu Y, Stice SL. Rapid Heterotopic Ossification with Cryopreserved Poly(ethylene glycol-) Microencapsulated BMP2-Expressing MSCs. Int J Biomater. 2012;2012:861794. Epub 2012 Feb 7. PMID:22500171

12. Salisbury EA, Olmsted-Davis EA, Davis AR. Adverse events and bone morphogenetic protein 2. Spine J. 2011 Aug;11(8):802. No abstract available. PMID:21925422
13. Salisbury E, Hipp J, Olmsted-Davis EA, Davis AR, Heggeness MH, Gannon FH. Histologic identification of brown adipose and peripheral nerve involvement in human atherosclerotic vessels. Hum Pathol. 2012 Jun 27. [Epub ahead of print] PMID:22748303
14. Mumaw J, Jordan ET, Sonnet C, Olabisi RM, Olmsted-Davis EA, Davis AR, Peroni JF, West JL, West F, Lu Y, Stice SL. Rapid Heterotopic Ossification with Cryopreserved Poly(ethylene glycol-) Microencapsulated BMP2-Expressing MSCs. Int J Biomater. 2012;2012:861794. Epub 2012 Feb 7. PMID:22500171
15. Saik, J.E., Gould, D.J., Keswani, A.H., Dickinson, M.E., West, J.L., "Biomimetic Hydrogels with Immobilized EphrinA1 for Therapeutic Angiogenesis." Biomacromolecules, 2011, PMID: 21639150.
16. Slater, J.H., Miller, J.S., Yu, S.S., West, J.L., "Fabrication of Multifaceted Micropatterned Surfaces with Laser Scanning Lithography". Advanced Functional Materials, 2011, 21, DOI: 10.1002/adfm.201100297.
17. Leslie-Barbick, J.E., Saik, J.E., Gould, D.J., Dickinson, M.E., West, J.L., "The promotion of microvasculature formation in poly(ethylene glycol) diacrylate hydrogels by an immobilized VEGF-mimetic peptide.", Biomaterials, 2011, PMID: 21612821
18. Stephens-Altus, J.S., Sundelacruz, P., Rowland, M.L., West, J.L., "Development of bioactive photocrosslinkable fibrous hydrogels.", J Biomed Mater Res A., 2011, PMID: 21548066.
19. Strong, L.E, West, J.L., "Thermally responsive polymer-nanoparticle composites for biomedical applications." Wiley Interdiscip Rev Nanomed Nanobiotechnol., 2011, PMID: 21384563
20. Durst, C.A., Cuchiara, M.P., Mansfield, E.G., West, J.L., Grande-Allen, K.J., "Flexural Characterization of Cell Encapsulated PEGDA Hydrogels with Applications for Tissue Engineered Heart Valves." Acta Biomater., 2011, PMID: 21329770.
21. Bahney, C.S., Hsu, C.W., Yoo, J.U., West, J.L., Johnstone, B., "A bioresponsive hydrogel tuned to chondrogenesis of human mesenchymal stem cells." FASEB J., 2011, PMID: 21282205.
22. Leslie-Barbick, J.E., Shen, C., Chen, C., West, J.L., "Micron-Scale Spatially Patterned, Covalently Immobilized Vascular Endothelial Growth Factor on Hydrogels Accelerates Endothelial Tubulogenesis and Increases Cellular Angiogenic Responses." Tissue Eng Part A. 2010. PMID: 20712418,
23. Saik, J.E., Gould, D.J., Watkins, E.M., Dickinson, M.E., West, J.L., “Covalently Immobilized Platelet Derived Growth Factor-BB Promotes Angiogenesis in Biomimetic Poly(ethylene glycol) Hydrogels”, Acta Biomater 7:133-43, 2010 PMID: 20801242.
24. Hoffmann, J.C., West, J.L., “Three-dimensional photolithographic patterning of multiple bioactive ligands in poly(ethylene glycol) hydrogels”, Soft Matter, 6: 5056-63,2010, DOI: 10.1039/c0sm00140f.
25. Cuchiara, M.P., Allen, A.C., Chen, T.M., Miller, J.S., West, J.L., “Multilayer microfluidic PEGDA hydrogels”, Biomaterials, 31:5491-7, 2010. PMID: 20447685.
26. Moon, J.J., Saik, J.E., Poché, R.A., Leslie-Barbick, J.E., Lee, S.H., Smith, A.A., Dickinson, M.E., West, J.L., “Biomimetic hydrogels with pro-angiogenic properties”, Biomaterials, 31:3840-7, 2010. PMID: 20185173.
27. Nemir, S., Hayenga, H.N., West, J.L.,“PEGDA hydrogels with patterned elasticity: Novel tools for the study of cell response to substrate rigidity”, Biotechnol Bioeng., 105: 636-44, 2010. PMID: 19816965.
28. Nemir, S., West, J.L., “Synthetic Materials in the Study of Cell Response to Substrate Rigidity”, Ann Biomed Eng., 38:2-20, 2010. Epub 2009, PMID: 19816774. Review.
29. Leslie-Barbick, J.E., Moon, J.J., West, J.L., “Covalently-immobilized vascular endothelial growth factor promotes endothelial cell tubulogenesis in poly(ethylene glycol) diacrylate hydrogels”, J Biomater Sci Polym Ed., 20:1763-79, 2009. PMID: 19723440.
30. Moon, J.J., Hahn, M.S., Kim, I., Nsiah, B.A., West. J.L., “Micropatterning of Poly(Ethylene Glycol) Diacrylate Hydrogels with Biomolecules to Regulate and Guide Endothelial Morphogenesis”, Tissue Eng Part A, 15:579-85, 2008. PMID: 18803481.

Pending patents:

International Patent Application No.: PCT/US2010/58603
Title: Methods and Compositions for Bone Formation
Filling Date: December 1, 2010
Inventor: Elizabeth A. Davis, *et al*

Conclusions:

We have demonstrated the ability of both the hydrogel encapsulated cells as well as the cells directly injected to induce heterotopic bone formation when implanted in the paraspinous musculature. This heterotopic bone formation can then rapidly fuse to the adjacent skeletal bone, even in the absence of injury or decortification. In both cases when cells are directly injected or hydrogel encapsulated the heterotopic bone can form a bridge between two or more vertebra to create spine fusion as demonstrated by histological, radiological and biomechanical analysis. We have optimized the hydrogel encapsulation and structures, to develop a method which rapidly generates small microbead structures, consisting of 1-100 AdBMP2 transduced cells. These encapsulation does not reduce transgene expression, or in this case secretion of the BMP2. It can freely diffuse into the media, similarly to the unencapsulated cells. Another benefit to the material is that there is absolutely no cell toxicity associated with the process. The cells tolerate the encapsulation, and have similar short term viability to the unencapsulated counterparts. Further, in vivo the hydrogel encapsulation actually protects the cells from targeted degradation, most likely due to the first generation adenovirus used in the transduction. Thus our data clearly shows that both cell lifespan and transgene expression are significantly expanded in vivo when cells are first encapsulated.

Interestingly, the microspheres not only lead to heterotopic ossification similar to the unencapsulated, but they appear to be capable of undergoing the same patterning, that is essential for long term viability of the HO and fusion. In our studies, we documented the patterning of the newly forming HO, to encompass the entire set of microbeads, but not invade any of the peripheral tissues, accept at points where it fused with the skeletal bone. Further, the interior amazingly functioned differently than the exterior which rapidly formed a thick layer of bone. The interior housed a tentative marrow cavity, with blood vessels, adipose, and nerves, suggesting that the normal skeletal bone architecture could be recapitulated even in the presence of the biomaterial. Finally we observed significant degradation and some removal-replacement of the material with bone, three weeks after delivery of delivery of the degradable sphere's encapsulating AdBMP2 transduced cell. This suggests that the material will slowly be removed without major disruption to the newly formed and fusing heterotopic bone. Thus, we have clearly demonstrated landmark steps in development of this therapy. HO can rapidly fuse into the vertebra without need for skeletal bone formation to create a stable fusion. Encapsulation of the cells in degradable hydrogel, allows for the cells to secrete BMP2 at designated locations. The new bone then forms around the periphery of the beads, and eventual within as the polymer degrades through cleavage of the protease sites. We are currently working on molding the microspheres into specific structures, implanting them and seeing if we can create specific shapes. With the ability to model specific structures, one could them provide an amazingly powerful tool for cranial facial reconstruction.

We have demonstrated the ability of the microspheres to protect the cells, and provide long term expression of the BMP2, even in when non-autologous cells were used. This provides significant advancement for manufacturing obstacles with other approaches in the literature. In our approach, the cells can be prequalified, and manufactured. Secondly, the transduction is transient, non-integrating, so there is no worry that the insertion of the transgene will lead to disruption of a critical gene, or that instability of the genome, may lead to long term problems such as cancer, which have been reported for other types of integrating gene therapy approaches. Further, encapsulation of the cells, provides additional safety, that cells expressing BMP2 will not try to form any structures of the bone. In other words, our system is totally transient. It rapidly produces the fusion, allowing the skeletal bone, to take over maintaining the structure, while any potential adverse effects of the therapy are eliminated. Incorporation of the foreign cells chronically expressing BMP, would lead to a significant potential for adverse reactions in the skeletal bone and surrounding tissues. This family of factors is highly regulated, and involved in key patterning pathways that govern interactions between multiple tissues and structures. Leaving the gene permanently expressed in foreign stem cell integrating into the bone, even at low levels could lead to a significant adverse long term outcome including chronic pain. Thus the ability to rapidly generate the fusion, and remove all the "foreign materials" so that the patient after healing is left only with their own cells, is a huge advantage.

Finally our work in the rat models, demonstrating that the allogenic primary cells, we have manufactured as a specific lot, and will use for completion of the efficacy testing, consistently produces bone formation at the targeted location, without causing any inflammatory reaction. This is the first time anyone has shown the ability to reproducible generate heterotopic ossification at a targeted location, in wild type outbred rats. From these data, we are nearing the end of phase 1 for this project, in that we now have a product that we can readily manufacture, and will reproducibly form HO, without adverse reaction. To further, these studies we are currently completing the efficacy data collection under GLP conditions, in wild type outbred rats. We

have also working on confirming that the material will maintain its efficacy after cryopreservation of the material which will be critical to manufacturing and implementation of the therapy.

Completion of this project has and will continue to significantly advance the current state of gene therapy in this field by eliminating the search for an optimal osteoprogenitor cell, scaffolding, and allow for rapidly translation to the clinic. But even more importantly, it would offer a non-invasive alternative to current treatments for degenerative spine disorders. Posterolateral spine fusion, which normally results in 500-1000 cc of blood loss as well as a 5 to 7 day hospital stay and a recovery period of up to a year, could be performed on an outpatient basis with this minimally invasive procedure, without concern over undue morbidity. This technology would benefit a broad age range of patients, and greatly reduce treatment costs as well as loss work time. Our proposed method has the potential to improve the safety of current spine surgery techniques by offering a safe and efficacious outpatient alternative to surgery, which will eliminate patient down time, rehabilitation and associated risks with the current process. Finally it will provide an opportunity to patients who require spine fusion but are not candidates for major surgery.

References:

1. Z. Lazard, M. Heggeness, R. M. Olabisi, C. Hsu, J.A. Hipp, F. Gannon, A. R. Davis, J. L. West, and E. Olmsted-Davis. Cell Based Gene Therapy for Repair of Critical Size Defects in the Rat Fibula. J Cell Biochem. 2011 Jun;112(6):1563-71. [Epub ahead of print.] PMID:2134448.
2. Chih-Wei Hsu, Ronke M. Olabisi, Alan R. Davis, Elizabeth A. Olmsted-Davis, Jennifer L. West. Cathepsin-K sensitive poly(ethylene Glycol) hydrogels for degradation in response to bone formation. J Biomed Mater Res A. 2011 Apr 26. [Epub ahead of print] PMID: 21523904.
3. Malavosklish Bikram, Christine Fouletier-Dilling, John A, Hipp, Francis Gannon, Alan R. Davis, Elizabeth A. Olmsted-Davis, and Jennifer L. West (2007) Endochondral Bone Formation from Hydrogel Carriers Loaded with BMP2-Transduced Cells. Ann Biomed Eng. 35(5):796-807 PMID: 17340196.
4. Ronke M. Olabisi, Zawaunyka Lazard, Mary Hall, Eva Sevick, John A Hipp, Alan R. Davis, Elizabeth A. Olmsted-Davis and Jennifer L. West. Hydrogel microsphere encapuslation of a cell based gene therapy system; increases cell survival, transgene expression, and bone volume in a model of heterotopic ossification. Tissue Eng Part A. 2010 Dec;16(12):3727-36. Epub 2010 Sep 1 PMID: 20673027.
5. Ronke M Olabisi, Zawaunyka Lazard, Michael Heggeness, Kevin M Moran, John A Hipp, Ashvin Dewan, Alan R. Davis, Jennifer L. West and Elizabeth A. Olmsted-Davis. An Injectable Method for Spine Fusion. Spine J. 2011 Feb 1. [Epub ahead of print] PMID: 21292563.
6. Dilling CF, Wada A, Lazard Z, Salisbury E, Gannon F, Vadakkan T, Gao L, Hirschi K, Dickinson M, Davis AR, Olmsted-Davis E. (2009) Vessel Formation is Induced Prior to the Appearance of Cartilage in BMP2-Mediated Heterotopic Ossification. J Bone Miner Res. J Bone Miner Res. 2010 May;25(5):1147-56. PMID: 19839764.
7. E. A. Olmsted-Davis, F. H. Gannon, M. Ozen, M. M. Ittmann, Z. Gugala, J. A. Hipp, K. M. Moran, C. Fouletier-Dilling, S. Schmura-Martin, R. W. Lindsey, M. H. Heggeness, M. K. Brenner and A. R. Davis (2007) Hypoxic Adipocytes Pattern Early Heterotopic Bone Formation. Am J Path 170:620-632 PMID: 17255330.
8. C. Fouletier-Dilling, F. Gannon, E.A. Olmsted-Davis, Z. Lazard, M. Heggeness, J.A. Shafer, J.A. Hipp, and A.R. Davis. (2007) Efficient and Rapid Osteoinduction in an Immune Competent Host. Hum Gene Ther 18(8):733-45 (Fast Track publication and Cover) PMID: 17691858.
9. Zhao KD, Yang C, Zhao C et al. Assessment of noninvasive intervertebral motion measurements in the lumbar spine. *J.Biomechanics* 2005;38:1943-6.
10. Hipp JA, Wharton ND. Quantitative motion analysis (QMA) of the spine. In: Yue JJ, Bertagnoli R, McAfee PC et al., eds. *Motion Preservation Surgery of the Spine*. 1st ed. New York: Elsevier Health, 2008.
11. Ashvin K. Dewan, Rahul A. Dewan, Nathan Calderone, Angie Fuentes, ZaWaunyka Lazard, Alan R. Davis, Michael H. Heggeness, John A. Hipp, and Elizabeth A. Olmsted-Davis. Assessing Mechanical Integrity of Spinal Fusion by *in situ* Endochondral Osteoinduction in a Murine Modal J Orthop Surg Res. 2010 Aug 21;5:58. PMID: 2072719.